UNIVERSITY OF CALIFORNIA
RIVERSIDE

Polypyrrole-Functionalized Single-Walled Carbon Nanotube Gas Sensor Arrays

A Thesis submitted in partial satisfaction
of the requirements for the degree of

Master of Science

in

Chemistry

by

James Kakoullis, Jr.

August 2011

Thesis Committee:
Dr. Ashok Mulchandani Co-Chairperson
Dr. Wenwan Zhong Co-Chairperson
Dr. Quan Cheng

The Thesis of James Kakoullis, Jr. is approved:

_____

_____
Committee Co-Chairperson

_____
Committee Co-Chairperson

University of California, Riverside

ACKNOWLEDGEMENTS

I would first like to thank my family for all their love and support over these past years that I have attended graduate school. I could not have gotten to this point in my life without them.

I would also like to thank my graduate advisor. If it were not for him I would not be at this point.

I would also like to thank my lab mates, in particular: Sandra C. Hernández, Mahendra D. Shirsat, Tapan Sarkar and Sira Srinives

ABSTRACT OF THE THESIS

Polypyrrole-Functionalized Single-Walled Carbon Nanotube Gas Sensor Arrays

by

James Kakoullis, Jr.

Master of Science, Graduate Program in Chemistry
University of California, Riverside, August 2011
Prof. Ashok Mulchandani, Co-Chairperson
Prof. Wenwan Zhong, Co-Chairperson

The overall objective of this work is to fabricate and evaluate polypyrrole-single-walled carbon nanotubes hybrid structures based chemiresistive sensor arrays for sensitive, selective and discriminative sensing at room temperature of emissions from automobiles and industrial manufacturing. To conceive the sensor arrays single-walled carbon nanotubes (SWNTs) networks were aligned to bridge a 3 μm gap between a pair of prefabricated microelectrodes followed by coating with polypyrrole (PPY) with different dopants by electrochemical polymerization.

Initially, the sensor's synthesis conditions in terms of PPY thickness on SWNTs networks by varying the electropolymerization charge of the monomer pyrrole in presence of $LiClO_4$ dopant for the sensing of NH_3 was optimized. Using the optimized polymerization charge of 1 μC determined previously, arrays of SWNTs-PPY hybrid sensors were fabricated by replacing dopant $LiClO_4$ by L-camphor sulfonic acid, D-camphor sulfonic acid, *p*-toluene sulfonic acid and sodium dodecyl sulfonate.

Room temperature gas sensing performance of the PPY coated SWNTs network arrays to gases of environmental significance such as NH_3, NO_2, H_2S, SO_2, CO and CO_2 and volatile organic compounds such as benzene, toluene, ethyl benzene, p-xylene, methanol, n-hexane and acetone and humidity, was evaluated. Several folds enhancement in sensing performance was observed towards all the tested analytesfor hybrid devices when compared to bare SWNTs network devices. Differences in sensing performance were noticed for PPY coating with different dopants demonstrating the potential of using the array for discrimination of the tested analytes in a mixture by using chemometric techniques. The underlying sensing mechanism was also investigated by using the devices in chemFET mode configuration.

TABLE OF CONTENTS

LIST OF FIGURES

LIST OF TABLES

CHAPTER 1: BACKGROUND

1.1 Motivation

The main goal of this research was to develop a polypyrrole (PPy)-Single-Walled Carbon Nanotubes (SWNT) hybrid gas sensor on the nano-scale that would then be used, by changing the dopant, to create a sensor array. This was accomplished in three steps. The first step was done by optimizing the hybrid against an analyte that was known to respond well against both PPy and SWNT. The analyte chosen was ammonia (NH_3). Other reasons that this analyte was picked are discussed in section 1.2. After the hybrid was optimized against NH_3 it was then tested against other analytes. These other analytes were low molecular weight gases, volatile organic compounds (VOCs), and relative humidity (RH). Finally in order to create an array of responses, the dopant was changed from the original $LiClO_4$ to others. When coupled to pattern recognition software, this array of responses will eventually lead to identification of numerous gases. All of this will eventually lead to the development of what has been called an electronic nose. This term was first coined in 1988 and was described as "an instrument which comprises an array of electronic chemical sensors with partial specificity and appropriate pattern recognition system, capable of recognizing simple or complex odors"[2]

The research plan then is to first develop a PPy-SWNT sensor with $LiClO_4$ as the dopant through the optimization of thickness, by changing the charge that the PPy is applied. The sensor will be optimized for response against the gas NH_3. After this is done the optimized sensor will then be tested against different analytes. This will give a pattern of

responses. Once this is completed the same conditions will be applied to create new PPy-SWNT sensors by changing the dopant. This will have the impact of changing the pattern of response of the new sensors by changing the sensitivity and selectivity.

1.2 Gas Sensor

To begin, a sensor is a device that can measure an analyte's concentration. It is made of two main components. One is a sensing element that upon exposure to the analyte changes one of its physical properties, in this work resistance, in a measurable manner. The other component is a transducer that converts the resulting change into a quantifiable electrical signal.

A sensor is judged by a number of criteria:

Sensitivity: The slope of the calibration curve of the anaylte of interest.

Selectivity: The ability to differentiate the analyte of interest from other compounds/chemicals in the sample.

Response Time: The time required for the signal to achieve 90% of the full response.

Recovery Time: The time required for the signal to return to 90% of the original state.

Lower Detection Limit: The minimum concentration that can be detected.

Upper Detection Limit: The maximum concentration that can be detected.

Dynamic Range: A range that extends from the lower detection limit until the range is no longer linear.[3]

In this work a gas sensor is simply a sensor in which the analyte is gas. The specific type of sensor and mode of sensing were chemiresistors and conductometric sensing. In addition a chemical field effect transistor (chemFET) was used to probe the mechanism of sensing. In a chemiresistor the sensing element/transducer bridges the source and drain through which the current passes. In the research reported here, the sensing element/transducer is the PPy-SWNT hybrid. Specifically the PPy is the sensing element while the SWNT is the scaffolding for the PPy and, thus, the transducer. So when analyte binds to the PPy, this action causes either a donation or withdrawal of electron density, which results in a resistance change. A third possibility is that the analyte can cause swelling, which causes the resistance to change in the PPy. The change in resistance is then transferred to the SWNT and then passed along through the source and drain. A similar sequence of events occurs with the chemFET except there is a second current being applied, which acts to modulate or gate the flow of current coming through the source and drain. This acts as a sort of tap for the current in much the same way as a faucet controls the flow of water. When the current is applied from underneath this is called backgated chemFET (Figure 1.1)

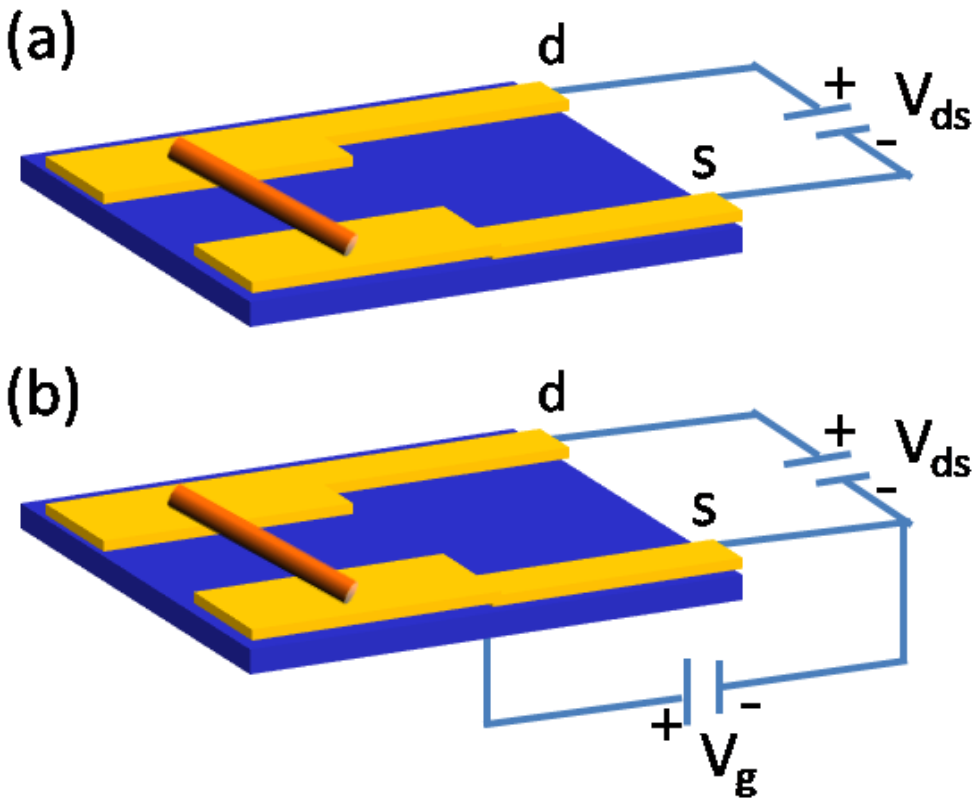

Figure 1.1 Schematic of **(a)** chemiresistor and **(b)** chemFET sensors. s: source, d: drain, V_{ds}: drain-source bias, V_g: gate bias.

Also in this work the gas that the hybrid was optimized against was NH_3. Now ammonia does respond well against PPy and SWNT. But it is also an important industrial compound. Ammonia is one of the oldest known compounds in the world and is the second most produced[4, 5]. The majority is used for fertilizer production; and the rest is used primarily in pharmaceuticals, plastics, explosives, and as a refrigerant[4]. However, NH_3 can be quite harmful: people are generally able to perceive NH_3 levels of 0.5 to 3 ppm, the Permissible Exposure Limit (PEL) is 50 ppm[6] and exposure equal to or greater than 5,000 ppm results in death. NH_3 is classified as an irritant and corrosive acting on the mucous membranes, with the pulmonary system being its primary target[4]. It can be quantified by various means: gas chromatography, infrared absorption, heat of neutralization, acidimetry and volumetric analysis by absorption, thermal conductivity, electrical conductivity, and density measurements (for NH_4OH). All of these techniques have the same fundamental limitations[4]. They can be labor and/or instrument intensive, requiring highly trained personnel to run and maintain expensive instruments that either can't give real-time data or are not portable. Thus, what is needed is a highly sensitive, reliable, easy to operate, low-cost and portable instrument that would yield real-time data. So there is a niche for a new device that will fill this gap, and that is where the sensor comes into play. Thus, because of its importance, NH_3 was chosen to have a more effective means of detection developed for it; and, because of its advantages, a sensor was chosen over other methods of detection.

1.3 Single-Walled Carbon Nanotubes (SWNT)

Carbon nanotubes are allotropes of carbon such as diamond and graphite. They were first discovered by Ijima in 1991. There are two classes of carbon nanotubes: Single-Walled Carbon Nanotubes (SWNT) and Multi-Walled Carbon Nanotubes (MWCT). In both cases a graphene sheet is warped around and covalently bonded to create a hollow cylinder. What distinguishes the two is that MWCT are nested within one another coaxially (with an intercylinder spacing of 3.4 Å) while in SWNT there is just a single tube with an average diameter of 1 to 5 nm [7].

SWNT can be further subdivided based on how the graphene sheet is wrapped. Depending on the lattice vector on which they are rolled and their diameter, three different types of SWNTs are possible. These are armchair, zigzag and chiral. The armchair SWNT are metallic in nature while the other two are semiconducting in nature. The semiconducting SWNT are p-type in character meaning that holes are the main charge carriers. MWNT are metallic in nature, the same as the armchair SWNT. (Figure 1.2)[8].

SWNT possess various novel properties that have made them a focus of research: electronic stability, thermal stability, and chemical inertness. They also have tensile strength that is 5 times that of steel. Most important to this work, SWNT have been used as sensing elements in the past. Because of these properties, they have already been used as nanogas sensors. These unfunctionalized SWNT have been applied as sensors for the detection of small molecules and dilute chemical vapors[9-14]. It has been known since the

beginning of sensor work with SWNT that they respond to NH_3[9]. Considerable effort has gone into improving the sensitivity of SWNT to NH_3[9, 15, 16]. Currently, the best response of bare SWNT is 5 ppm in detecting NH_3. SWNT, though, lack the selectivity and

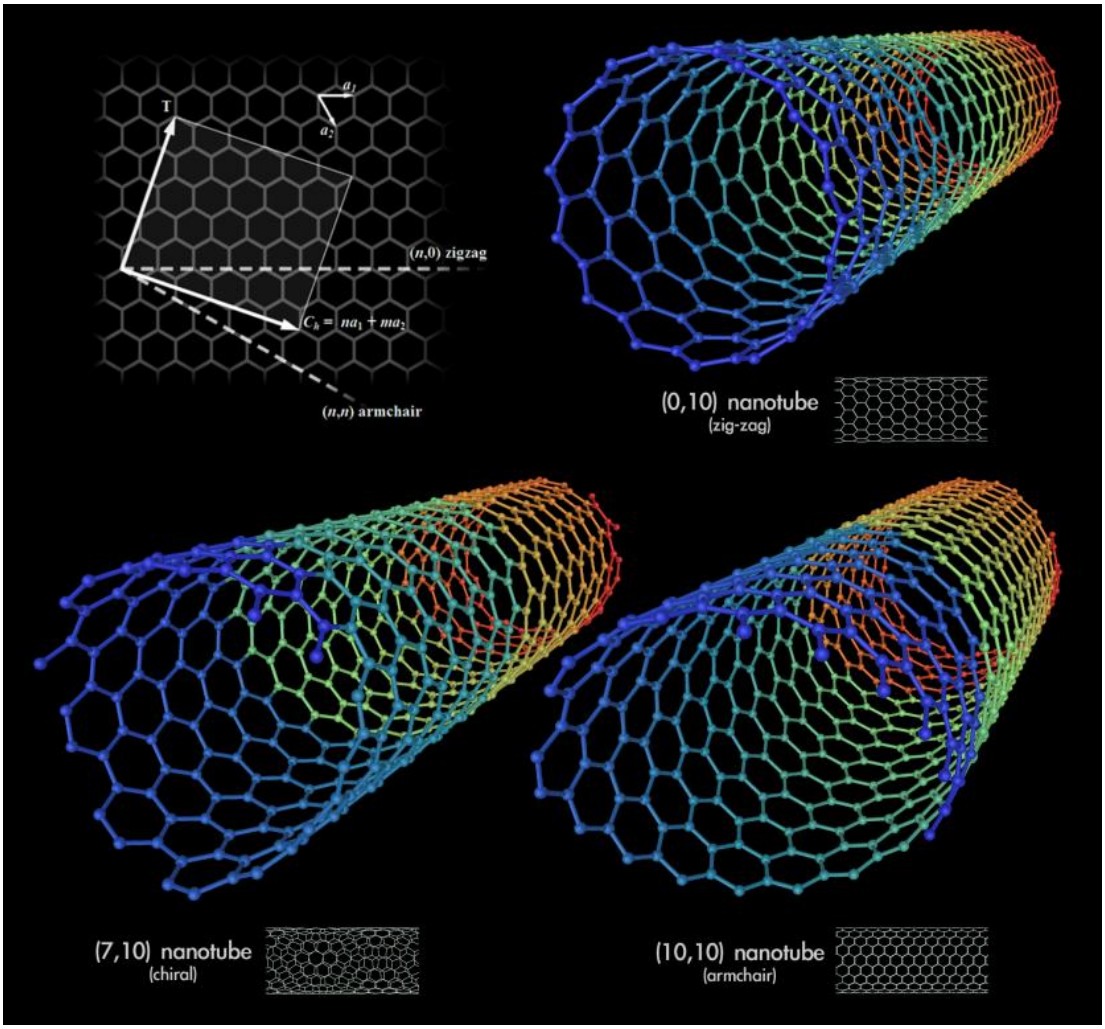

Figure 1.2 Different types of SWNT, A graphite sheet (top left), zig-zag (top right), chiral (bottom left), and armchair (bottom right) source http://en.wikipedia.org/wiki/Carbon_nanotube#Single-walled

sensitivity at lower concentration ranges to be fully implemented as reliable sensors. It has been shown in the past that by functionalizing SWNT with materials that show sensitivity towards analytes of interest, a synergistic effect in the resulting hybrid is created[17-20].

SWNT can be classified as 1-D nanostructures. They have distinct and notable advantages over 2-D nanostructures such as planar films. The diameters of these nanostructures are comparable to those of the analytes being sensed. Binding of an analyte to the surface of 1-D nanostructures can lead to either depletion or accumulation of carriers in the "bulk" of the nanometer diameter structure versus only in the surface region of a planar device, giving rise to large resistance/conductance changes (Figure 1.3). In addition, the direct conversion of chemical information into an electronic signal

can take advantage of existing low-power microelectronic technology and lead to massive multiplexed devices of small size. Finally, the ultra-small size of the nanostructures makes it possible to develop both high-density arrays of individually addressable nanostructures for simultaneous analysis of a range of different species and massive redundancy to increase the accuracy of the measurements[21]. All of these, points make SWNT ideal for construction of a nanogas sensor. What is missing is a way to increase the sensor's sensitivity

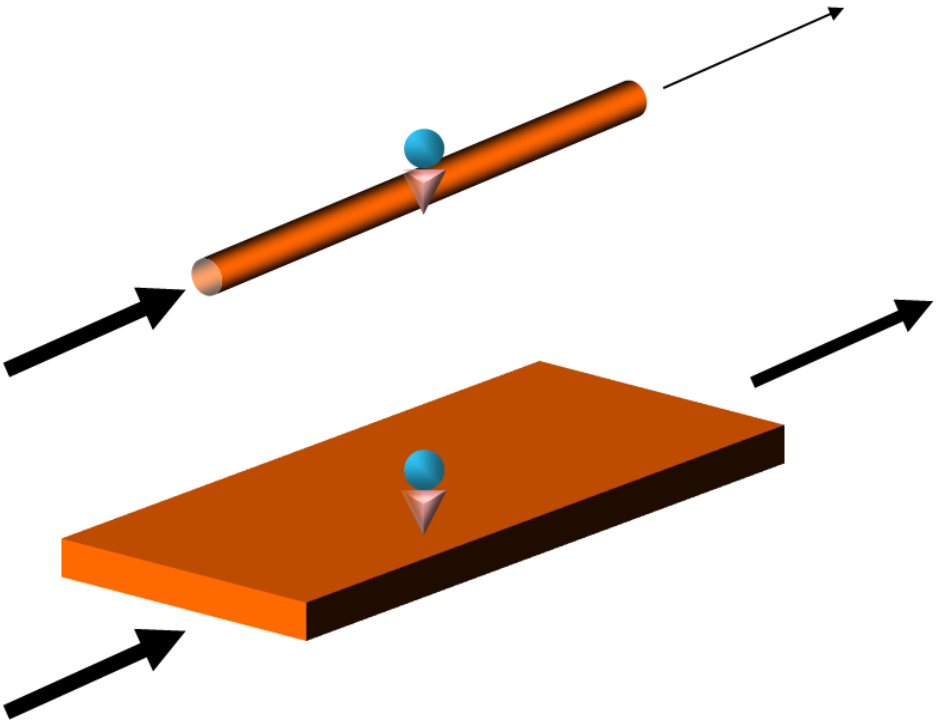

Figure 1.3 Schematic of 1-D nanostructure versus 2-D thin film, where arrows represent the charge carriers and density, blue sphere denotes the analyte and triangle denotes the depletion region.

1.4 Polypyrrole (PPy)

Pyrrole is a heterocyclic aromatic organic compound. It can readily be polymerized to form polypyrrole (Figure 1.4). The nature of this polymerization is either chemical or electrochemical. The polymer is intrinsically insulating but can be made to be conductive by "doping" with a counter-anion. This now conducting polymer (CP) has a conductivity ranging from that of a metal to that of a semiconductor. The amount depends on the amount and type of dopant used[22]. Polypyrrole also has environmental stability and good mechanical properties which are useful in this work.

Conductive polymer (CP) films have been applied as electrochemical sensors for some time[23-25]. They have been used in many different modalities of sensing, such as conductometric, amperometric, optical, piezoelectric crystal, and as field effect transistors (FETs) for the detection of various gases. CPs can also be synthesized electrochemically. The main benefits of this process are that, since the process is electrically initiated and driven, the polymer is localized at the working electrode surface and that the potential controls the rate while the charge controls the thickness. This process is low cost, has high throughput, is simple and is highly manufacturable. Also, the polymerization reaction can be terminated by shutting off the current. CPs films also have the advantage over say metals and metal oxides, which have to be operated at elevated temperatures, in that they can be operated at room temperature. CPs do have their drawbacks. When used as films, they lack the 1-D nanostructures' advantages. When CP wires are made, their diameters are much larger than those of SWNTs. Another

disadvantage of CPs is that over time they oxidize when exposed to oxygen. CPs thin films, specifically polypyrrole, PPy, have also been used for NH_3 gas sensors for some time, and considerable effort has gone into improving their sensitivity as well[26-30]. One of the best current responses is 8 ppm[28]. Therefore, CPs have limits when it comes sensitivity, as do SWNT[31-33]. So then by using both materials in concert to create a hybrid, the resulting material should have a higher sensitivity than either does on its own. Then by changing the dopant different selectivity can be introduced.

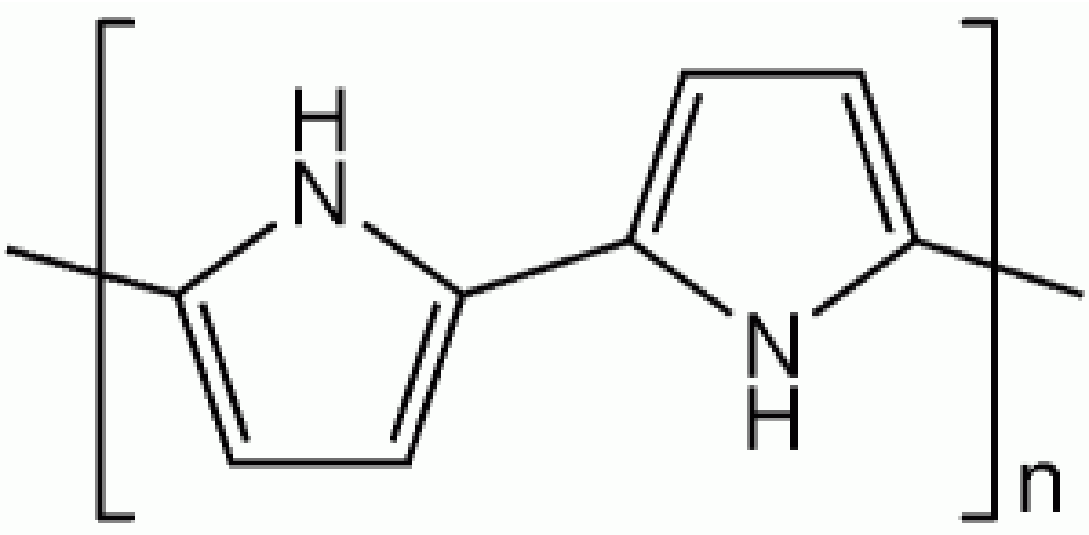

Figure 1.4 Polypyrrole, source
http://en.wikipedia.org/wiki/File:Polypyrrole.png

CHAPTER 2: MATERIALS AND METHODS

2.1 Materials and Equipment Used

The SWNT used were P3 SWNT-COOH 80 ~ 90 % purity, from Carbon Solution, Inc., Riverside, CA, USA. The reagents used were, pyrrole (Sigma Aldrich, reagent grade) which was vacuum distilled upon arrival and stored under N_2 in a freezer. All other reagents were used as received unless otherwise stated. The other reagents were *N, N*-dimethylformamide (Sigma Aldrich, Spectral grade), $LiClO_4$ (Acros Organic 99+ %, for analysis), D(+)-10-camphorsulfonic acid (D-CSA) (Acros organic 99 %), *p*-Toluenesulfonic acid monohydrate (pTSA) (Acros organic 99 %), , L(-)-Camphorsulfonic acid (L-CSA) (Acros organic 98 %), Sodium Dodecly Sulfate (SDS) (Fisher Biotech: Electrophoresis grade). Also used were the liquid reagents methanol (MeOH), ethanol (EtOH), acetone, n-hexane, benzene, toluene, ethyl benzene, and p-xylene. These were from Sigma-Aldrich and were reagent grade or better. The gases used for sensing were Zero-grade air (purity: 99.998 %), NH_3 (purity: 99.99 %), NH_3 (100 ppm) balanced in air, SO_2 (10 ppm) balanced in air, CO (100 ppm) balanced in air, CO_2 (1000 ppm) balanced in air, H_2S (40 ppm) balanced in air, and NO_2 (10 ppm) balanced in air. The gases used for annealing were ultra pure H_2 (99.999 %) and pre-purified N_2 (99.99 %). All of the gases were supplied by Airgas, USA.

For sonication a VWR Signature 50D Sonicator was employed. A Beckman J2-HS Centrifuge was used for centrifugation. For AC dielectrophoretic alignment a 4MHz Sweep/Function Generator was used. For annealing a Lindber Blue M Tube Furnace with a glass tube for the gases to flow through was used. CHI Model1202A Electrochemical

Analyzer was used for all electrochemical experiments such as chronoaperometry, cyclic voltammograms (CV), and Linear Sweep Voltammetry. Scanning Electron microscope (SEM), Philips XL30 FEG was used for imaging. An atomic force microscope (AFM) Innova, Veeco Instruments Inc. was also used. For determining the activation energy, a cold-finger cryogenic system Janis CCS-350SH, Wilmington, MA coupled to a Keithley 236 was used. A chemFET was set up using a Keithley 236 to monitor and control the voltage.

In the gas sensing the mass controllers used were from Alicate Scientific Incorporated, Tucson, AZ. The program employed to monitor the voltage was a custom Labview program. This was monitoring the output of a Fieldpoint Module (National Instruments, Austin, TX).

2.2 Preparation of SWNTs Suspension

A suspension of SWNT 0.2 mg/20 ml in *N*, *N*-dimethylformamide was made. This was produced by ultrasonically sonicating the sample for 90 min at ~ 45 W. Then the solution was transferred to a centrifuge tube and spun for 90 min at 31,000 g at a temperature of 23 °C. Finally 10 ml of the supernate was transferred to a new vial, which was sonicated for 60 min additionally at ~ 45 W.

2.3 Chip Preparation

A chip was prepared as stated previously (Figure 2.1)[1]. In brief by the use of standard lithographic patterning the electrodes of the sensor was microfabricated. This was done on a silicon substrate. To this substrate by the use of chemical vapor deposition (CVD)

one micron of SiO_2 film was deposited in a (100) orientation. This was done to insulate the substrate. After this step the electrodes were photo-lithographically defined. A Cr adhesion layer was placed down flowed by a 3000 Å thick Au layer by e-beam evaporation. The final step was the defining of the electrodes with lift-off techniques. The electrode gap between electrodes was set at 3 μm in distance[1].

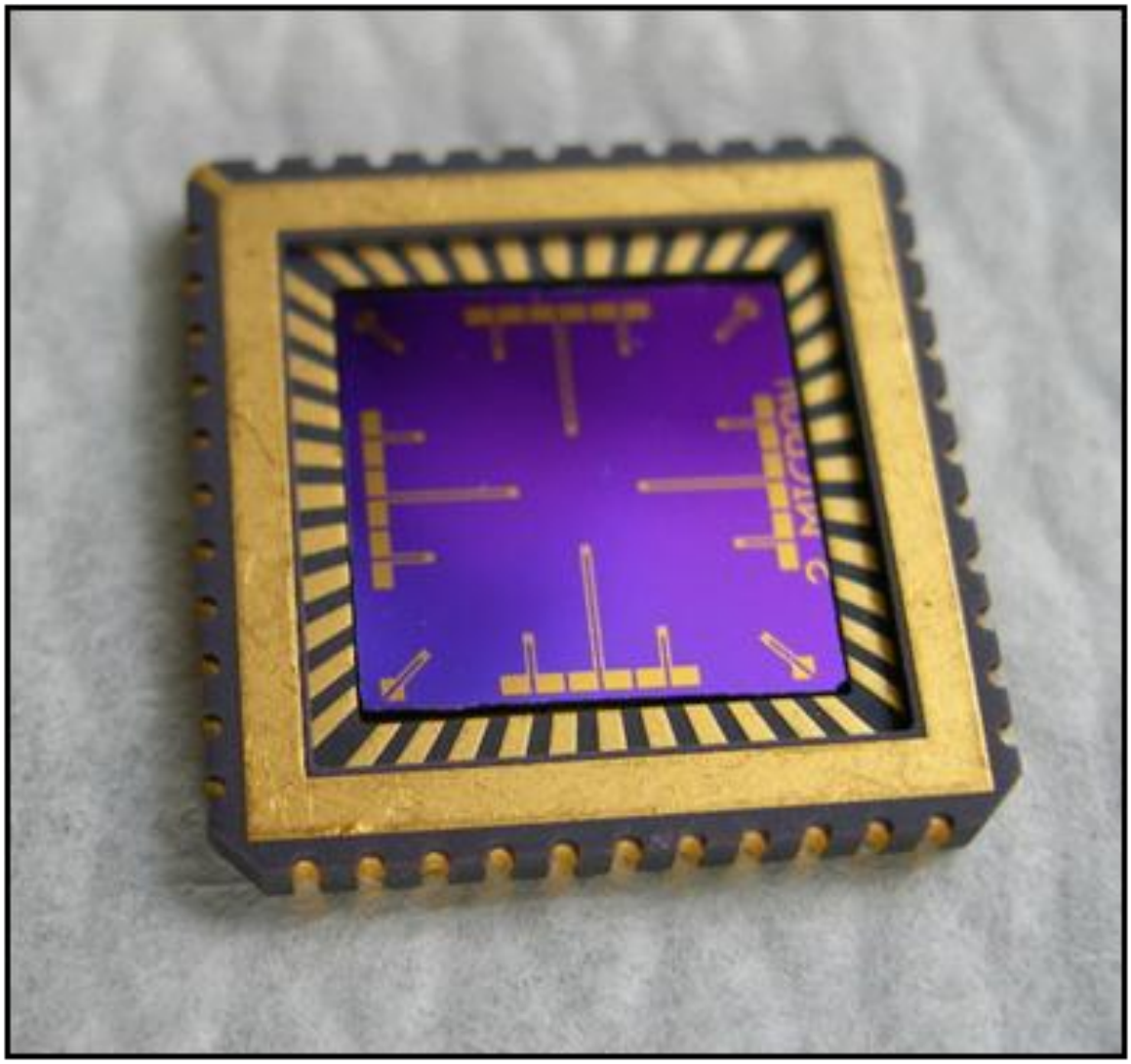

Figure 2.1 Image of 16 electrode 3 µm chip in holder, source [1]

2.4 AC Dielectrophoretic Alignment

The SWNT were aligned across the 3 μm electrode gaps via AC dielectrophoretic alignment by adding a 0.1 μL drop of SWNTs suspension and applying 3 V_{pp} and 4 MHz for ~ 5 s. The SWNT suspension was then washed away with nanopure water and then dried with N_2. This alignment process creates a SWNT device that would have better sensitivity than does a device made up of a random SWNT network.

2.5 Annealing

Alignment was followed by annealing at 300 ^oC for 1 h under 95 % N_2/ 5 % H_2 atmosphere. The annealing process improved the contact resistance between the Au contacts and the SWNT by reducing the resistance.

2.6 Electropolymerization

After SWNT annealing, electrochemical functionalization using chronoamperometry on the surface of the SWNT network was performed by addition of a 2 μL drop of a deoxygenated solution of 0.01 *M* pyrrole /0.1 *M* $LiClO_4$, using the Au pads as the working electrode, Pt wire as the counter electrode, and Ag/AgCl wire as a pseudo reference electrode. The thickness of the PPy coating was controlled by the amount of charge. Electropolymerization was initiated by applying 0.96 V on SWNT networks vs. Ag/AgCl reference to apply 1 μC, 5 μC, 10 μC and 15 μC of charge. After the deposition, the solution was washed away with nanopure water and then dried with N_2.

The samples were then placed in a vacuum desiccator to completely dry them. This was for the ammonia optimization part of the work. For the dopant part of the work all of the conditions were the same except the dopant/counter ion was changed from $LiClO_4$ to D-CSA, pTSA, L-CSA, and SDS. Also the charge was always kept at 1 μC.

2.7 Characterization

CV of unfunctionalized SWNT and PPy-SWNT-bundle hybrids in a 0.1 *M* $LiClO_4$ solution were taken. Linear Sweep Voltammetry was used to determine resistance by the current-voltage curve (I-V) of SWNT before and after functionalization. A SEM was used to qualitatively analyze the thickness of the PPy deposited on the SWNT. This analysis was quantified by AFM. By the use of a cold-finger cryogenic system, the thermal activation energy (E_a) was determined from the temperature-dependent I-V taken from 20 to 300 K. From these I-Vs an Arrhenius plot was constructed from which the E_a was determined over the range of 180 to 300 K.

To understand the underlying mechanism of sensing, the devices were set up as a back gated FET. The mechanism of sensing was explored by the use of chemFET. The 1 μC PPy-SWNT-bundle hybrid device was exposed to air and had its FET measurement done. This was repeated with NH_3 at a concentration of 10 ppm. This procedure was repeated with unfunctionalized SWNT.

2.8 Gas Sensing

For gas sensing studies, the system was set up as previously described (Figure 2.2)[34]. In brief, the chips were wire bonded to a chip holder that was then connected in series with a load resistance. The value of the load resistance matched that of the resistance of the gas sensor. The circuit then had a fixed voltage of 1 V applied to it. The electrical resistance of the sensor was determined by continuously monitoring the voltage over the load resistor and applying Ohm's Law. This would then give a read out in resistance of the sensor. Over the chip a 1.3 cm^3 glass dome was securely applied on top with an inlet and outlet for gas flow. Zero-grade air and NH_3 were used as the carrier and analyte gases, respectively, for the optimization experiments. For the other experiments Zero-grade air was the carrier and the analyte gases SO_2, CO, CO_2, H_2S, and NO_2 were used. The carrier gas was diluted with the analyte gas to obtain different analyte concentrations. To prepare the other gases, from liquids (methanol (MeOH), ethanol (EtOH), relative humidity (RH), acetone, n-hexane, benzene, toluene, ethyl benzene, and p-xylene), were placed in bubblers and the carrier gas was blown in at set concentrations. The resulting gases were then combined with carrier gas and diluted to the appropriate concentration. These flow rates of the analyte and carrier gas were managed by mass flow controllers. The total flow rate was maintained at 200 standard cm^3 min. The response and recovery were controlled to be 15 min. followed by 20 min. respectively for all gas sensing experiments unless otherwise stated[34].

A response recovery study was performed as outlined for gas sensing on the 1 μC PPy-SWNT-bundles hybrid, but the sensor was exposed to a set concentration of NH_3, e.g. 10 ppm, for a set period, e.g. 30 minutes, to saturate the hybrid. It was then monitored to determine how long the hybrid took to recover.

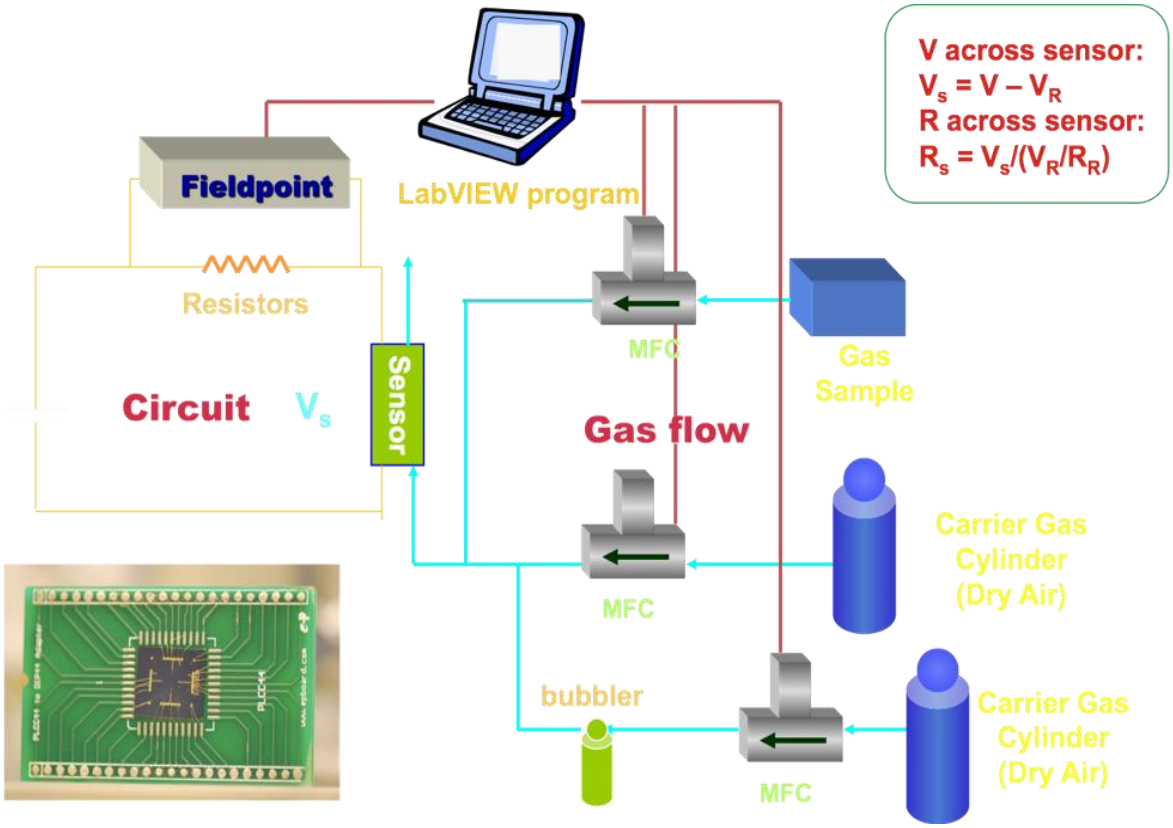

Figure 2.2 Schematic of gas sensing system.

CHAPTER 3: RESULTS AND DISCUSSION

3.1 Optimization of Ammonia gas sensor

3.1.1 Verification of Coating PPy on SWNT

The resistance of SWNT-bundles before and after functionalization was measured. All of the devices showed a small increase in resistance (data not shown). This trend has been noted before in other SWNT coated with PPy work[18].

Functionalized SWNTs-bundle hybrids, in contrast to the unfunctionalized SWNT, exhibited significantly higher output current; and the shape of the CV for the hybrid is similar to that observed for PPy in thin films, suggesting the successful deposition of PPy on the surface of the SWNT (Figure 3.1).

A SEM was used for qualitatively analysis of the thickness of the PPy deposited on the SWNT. As shown in Figure 3.2 the PPy thickness increased with increasing electrical charge.

This analysis was quantified by AFM. As the charge increased there was a corresponding increase in the diameter of SWNT-bundles (Figure 3.3).

Average diameters were as follows: 4.6 nm for bare, 11.1 nm for 1 μC, 24.9 nm for 5 μC, 35.9 nm for 10 μC and 49.8 nm for 15 μC. All of these data provide verification of PPy deposition on SWNT.

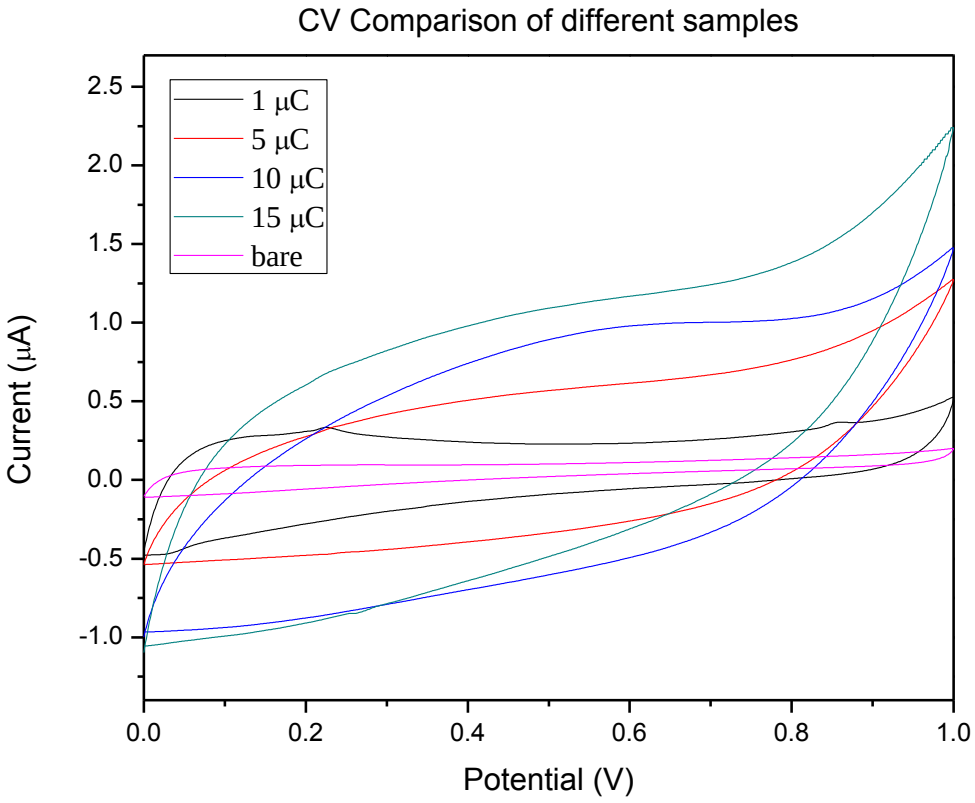

Figure 3.1 CV of PPy-SWNT-bundles hybrid and SWNT-bundles.

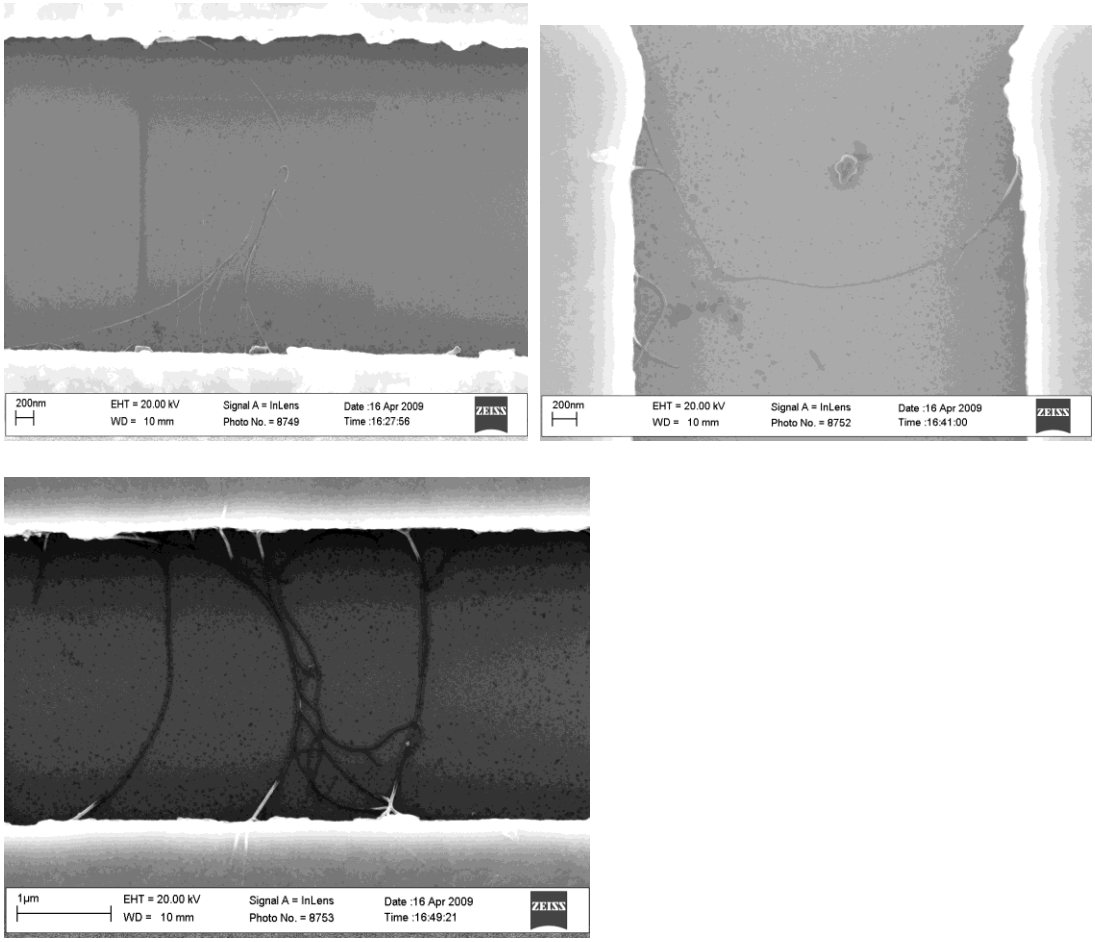

Figure 3.2 (a) SEM of bare SWNT-bundles (top left), (**b)** 1µC PPy-SWNT hybrid bundles (top right), and (**c)** 5µC PPy-SWNT hybrid bundles (bottom left).

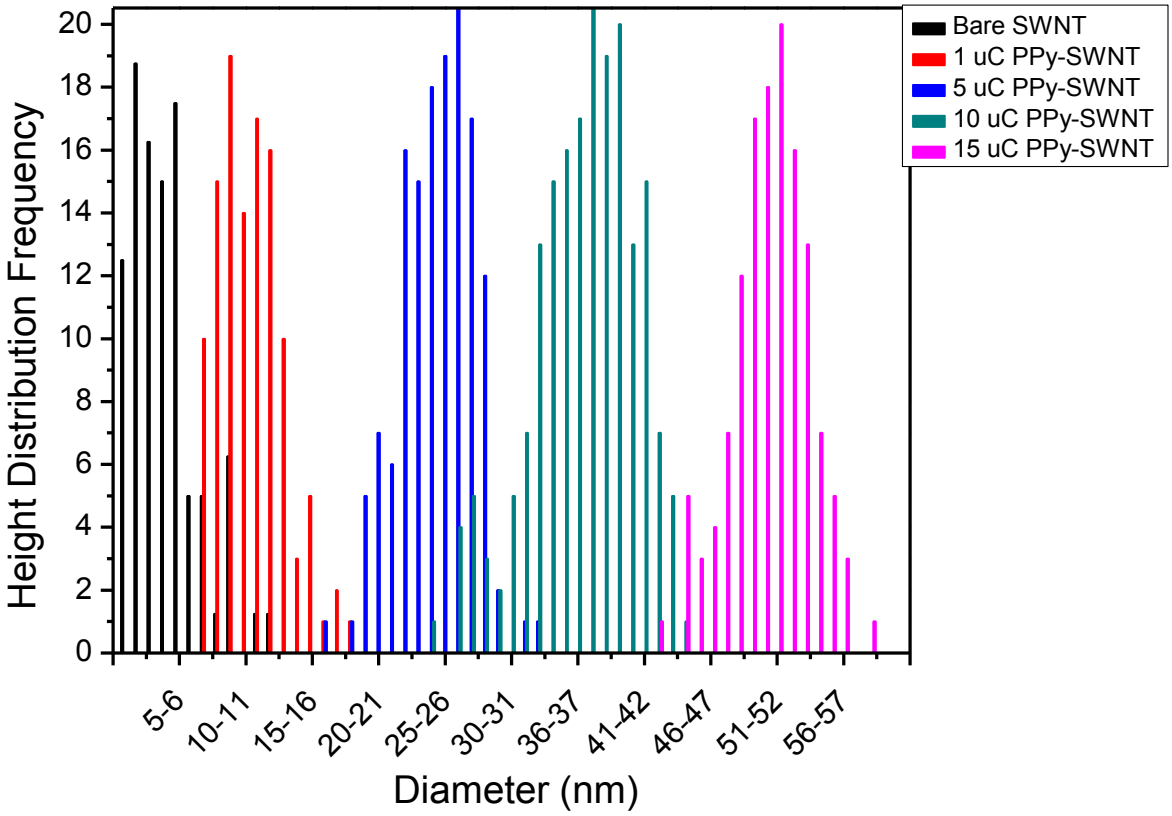

Figure 3.3 Height distribution frequencies of SWNT-bundles with different charges in nm.

3.1.2 Gas Sensing of Hybrid

Figure 3.4 shows the transient response of the 1μC PPy-SWNT-bundles hybrid. The dynamic range used was 1 ppb to 500 ppm. Figure 3.5 shows the calibration plot of the bare SWNT-bundles and PPy-SWNT-bundles hybrid sensors for NH_3. All of the responses, including bare SWNT, were collected; and their normalized resistance changes as a function of NH_3 concentration were compared. All of the functionalized SWNT-bundles hybrids responded better than bare SWNT-bundles in the lower range (1 ppb to 1 ppm). The bare SWNT-bundles, though, responded better than hybrids fabricated at applied charge 15 μC (10 ppm to 500 ppm). The functionalized SWNT-bundles, overall, responded better than bare SWNT-bundles; but as the applied charge increased, thus increasing the thickness of the PPy coating, the advantage of PPy functionalization decreases to the point where bare SWNT-bundles in some instances, e.g. 15 μC, are better (Figure 3.5 and 3.6). Overall, the hybrid fabricated at the applied charge of 1 μC had improved limit of detection, faster response rate, and greater sensitivity compared to bare SWNT-bundles. Figure 3.7 shows a response and recovery curve of a 1 μC PPy-SWNT-bundles hybrid to 10ppm NH_3. The device responded very quickly to the analyate reaching in twenty minutes, the exposure period, 120% response. This was to saturate the device. Then it was watched to see how long it would take for the device to recover. The device, after 1200 minutes, recovered to 41% of the original baseline value of 0. The hybrid, then, did not exhibit complete or faster recovery. Recovery can most probably be improved by heating the sample as has been shown in other SWNT gas sensors work[9].

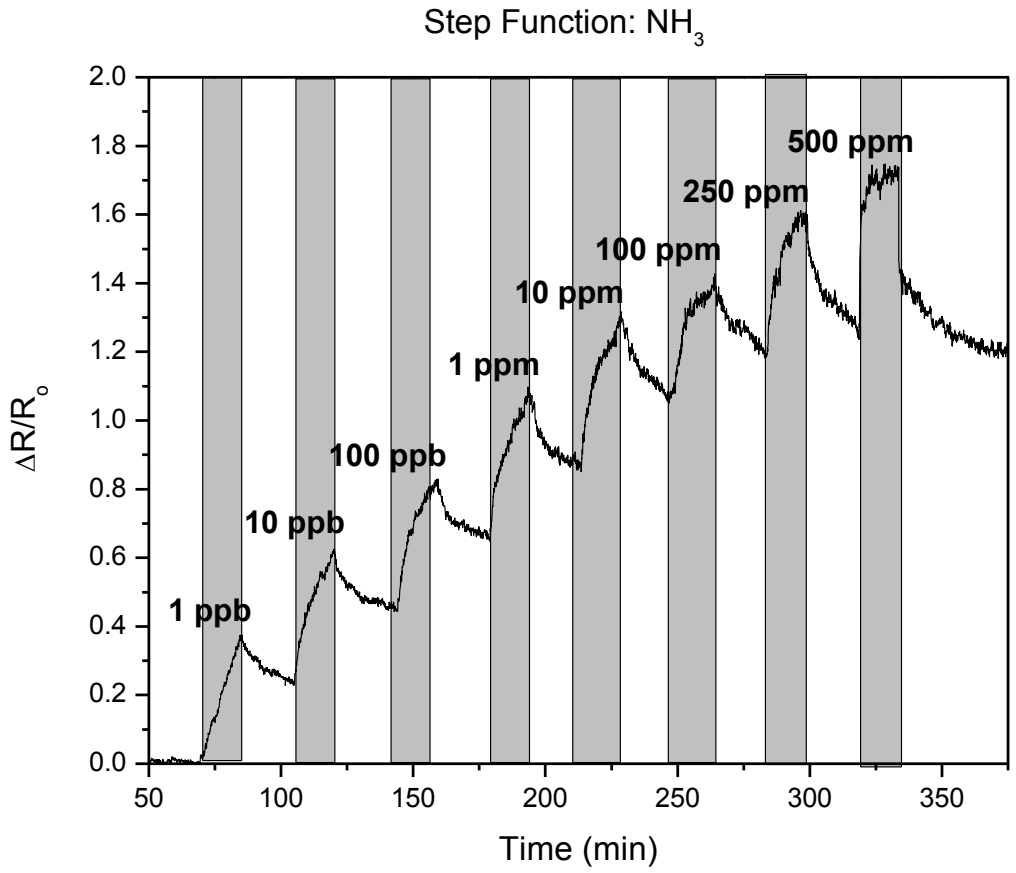

Figure 3.4 Transient response of PPy-SWNT-bundle hybrid with 1μC charge to NH_3 from 1 ppb to 500 ppm.

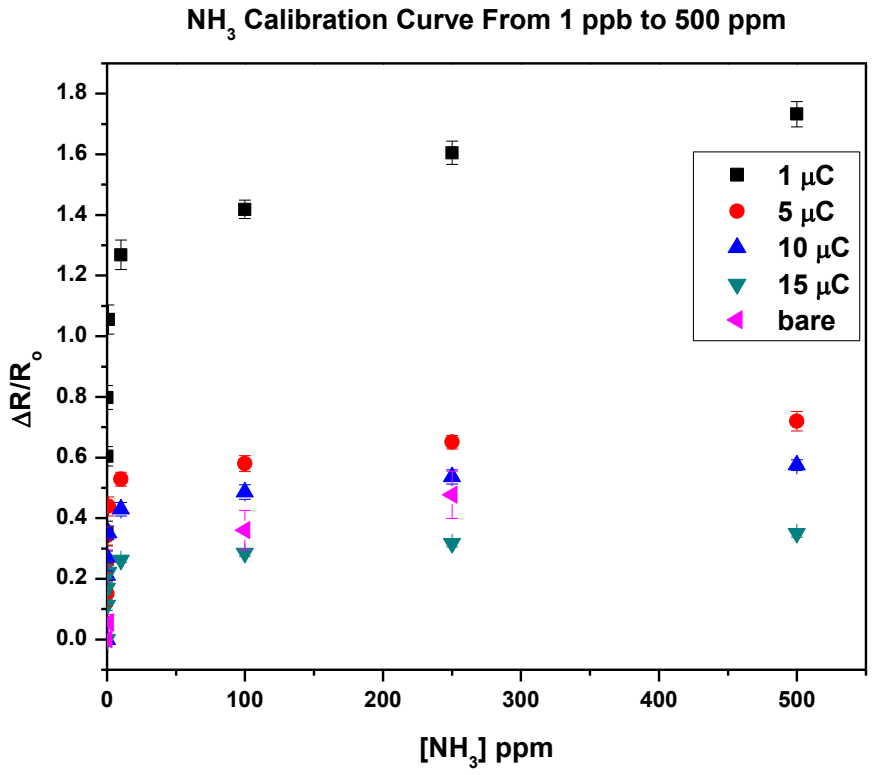

Figure 3.5 Calibration Curves of PPy-SWNT-bundle hybrid sensor and bare SWNT-bundle for NH_3 between 1 ppb and 500 ppm at room temperature.

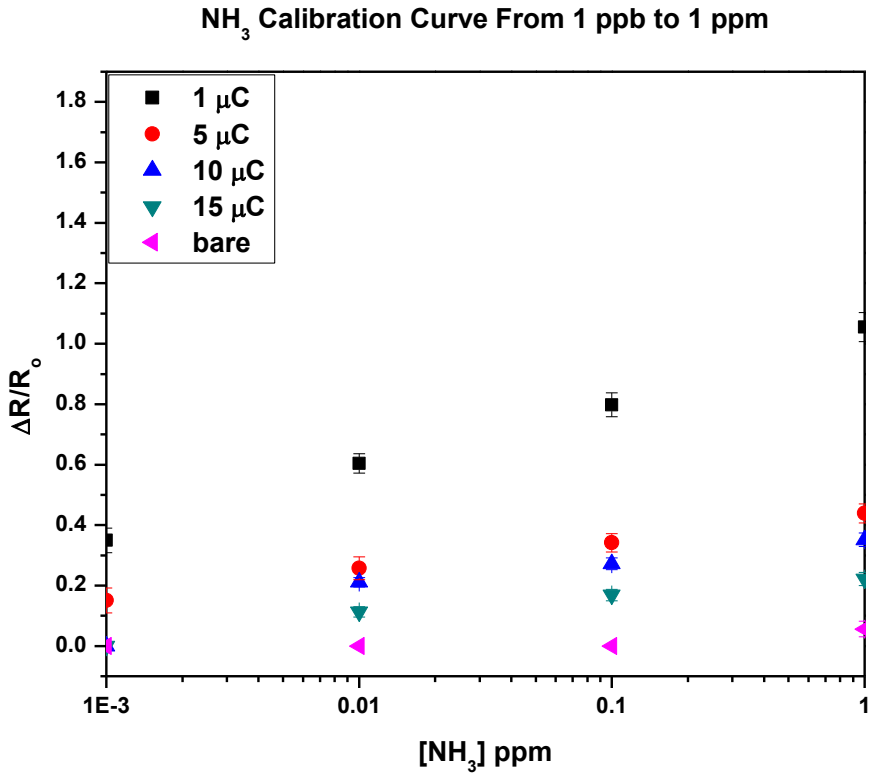

Figure 3.6 Calibration Curves of PPy-SWNT-bundle hybrid sensor and bare SWNT-bundle for NH_3 between 1 ppb and 1 ppm at room temperature.

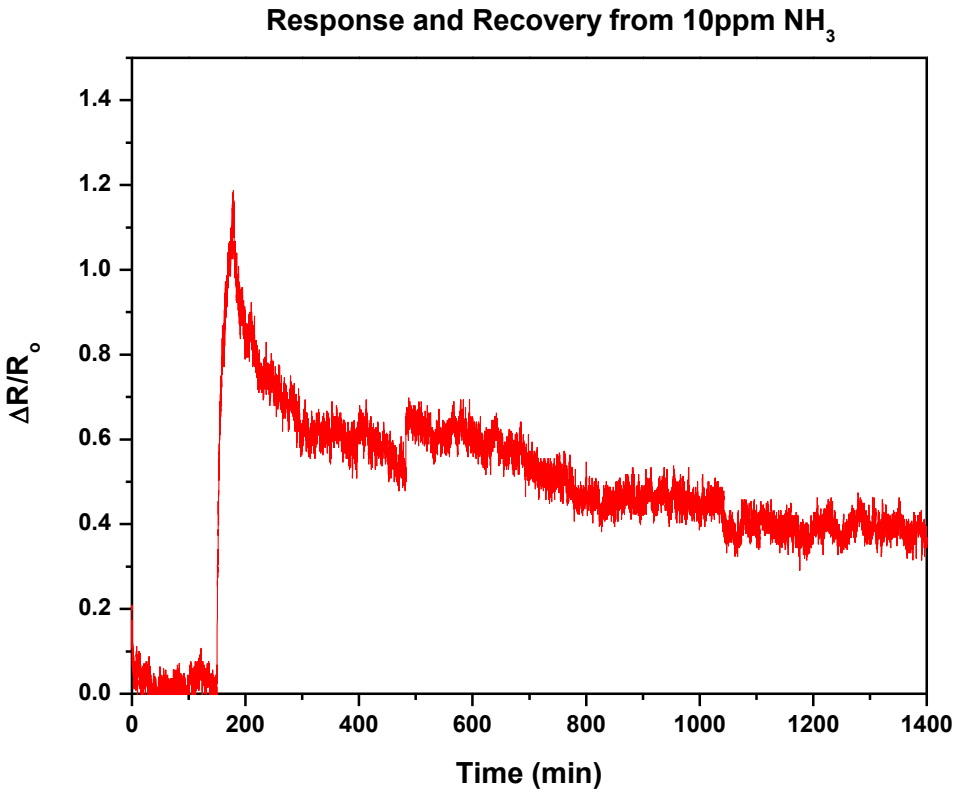

Figure 3.7 Response and Recovery of PPy-SWNT-bundle hybrid with 1 μC charge to 10 pm NH_3.

3.1.3 Mechanism of Sensing

The I_{DS}-V_g of the devices was taken. These curves indicate that these materials are p-type, meaning there is a deficiency of electrons and that holes are the charge carriers of these systems[35]. When the hybrid is exposed to NH_3, the I_{DS}-V_g, in comparison to the air I_{DS}-V_g, shows that there is a decrease in current, meaning that the valence band of PPy is shifting away from the Fermi band resulting in hole depletion and increased resistance (Figure 3.8)[9].

When comparing the hybrid in air to the hybrid exposed to NH_3, there is a small change in the slope of the curves. A change in slope indicates that the sensing mechanism is a Schottky effect, however, since the slope change is small, this is not the dominant mechanism, but rather the minor mechanism[36].

There is also a large change in threshold voltage between the two I_{DS}-V_g; this corresponds to a gate effect sensing mechanism, which is the dominant mechanism[36]. Bare SWNT-bundles had their sensing mechanism explored as well. This was done to see if the PPy coating changed the mechanism of sensing. It is known from previous work that the dominant sensing mechanism for bare SWNT-bundles is a Schottky effect[37]. In our work, though, the dominant sensing mechanism is a gate effect (data not shown).

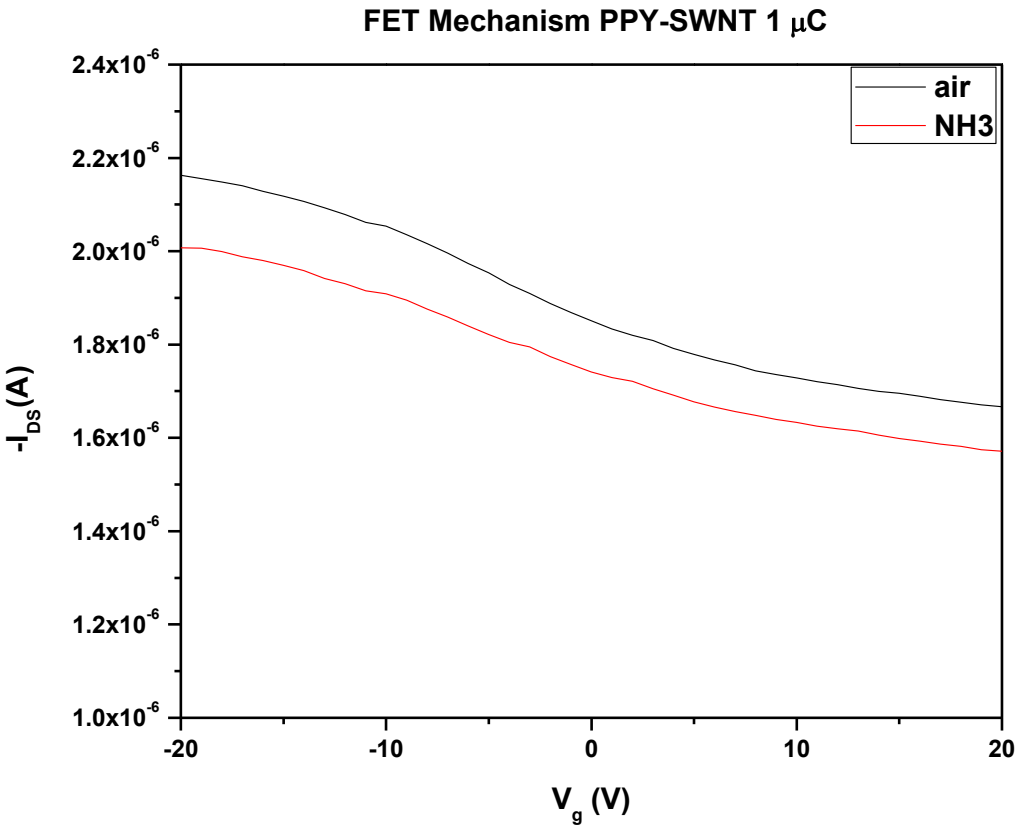

Figure 3.8 A representative I_{DS}-V_g of 1 μC PPy-SWNT bundle hybrids in air and NH_3.

The reason for the difference is that in the literature example metallic SWNT have been removed by burning, so only semiconducting SWNT are left[37]. The SWNT discussed in this report are a mixture of metallic and semiconducting SWNT. This is supported by activation energy (E_a).

3.1.4 Thermal Activation Energy Comparison

The E_a for a device was compared before and after functionalization for the 1 µC PPy-SWNT hybrid (Figure 3.9).

The E_a for the bare was 15.5 meV and increased after functionalization to 23.7 meV. This increase indicates that the material is becoming more semiconducting. The values for metallic SWNT and semiconducting SWNT are 5 meV and 29 meV respectively[38]. The value of 15.5 meV is between metallic and semiconducting, supporting the contention that this device is made up of a mixture of the two types. This helps explain why the mechanism is not a Schottky effect as was the case in the previous reports where the SWNT were all semiconducting[37].

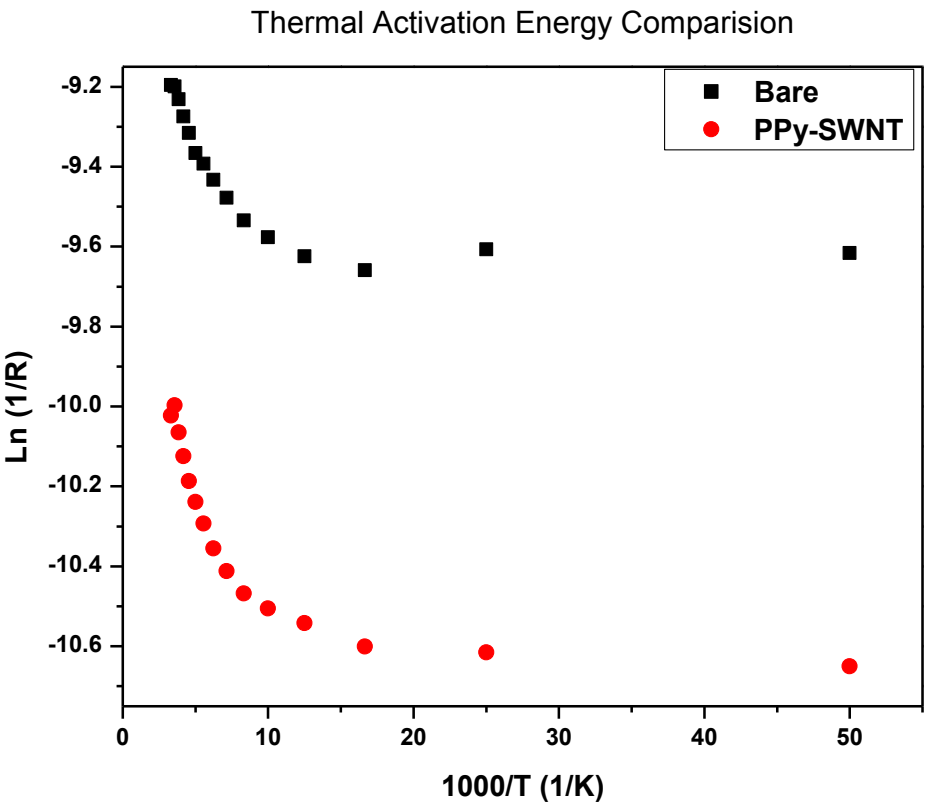

Figure 3.9 Thermal Activation Energy Comparison between Bare SWNT and PPy-SWNT 1 µC hybrids.

3.2 Effect of Dopant Change

3.2.1 Resistance

The resistance of SWNT-bundles before and after functionalization was measured. All of the devices after coating showed a small increase in resistance (data not shown). This trend has been shown before with PPy-SWNT devices[18].

3.2.2 Discussion of Analytes in General

After the optimization, the same charge was used but the dopant was changed. The reason for this was that it had already been determined that this was the optimized coating thickness of PPy on SWNT. By changing the dopant we wanted to be able to change the selectivity of the hybrid to the gases. This can be seen first off in the response to NH_3 (Figure 3.10). The difference between $LiClO_4$ and L-CSA, D-CSA, pTSA, and SDS is quite significant. $LiClO_4$ had a much higher response than the others.

The responses for the devices can be broken down into two categories according to molecular weight. The low molecular weight gases, i.e. NH_3, SO_2, CO, CO_2, H_2S, and NO_2 had responses in the ppm range with the exception of CO and CO_2, which did not respond. The high molecular weight gases, i.e. MeOH, EtOH, RH, acetone, n-hexane, benzene, toluene, ethyl benzene, and p-xylene, responded in the vapor pressure range. These gases, except RH, can also be classified as volatile organic compounds (VOCs).

Changing of the dopant in the PPy had the impact of changing the amount of response of the material from one analyte to another (Figure 3.10 and 3.11). This impact can also be seen if one examines the individual response of an analyte to a material (Figure 3.12).

The response of the differently doped PPy to RH can be seen. At 75 % RH, SDS responded the highest (50 % on average) followed by $LiClO_4$, L-CSA, D-CSA, pTSA (5 % on average), and bare SWNT. So we have reduced the impact of RH on the hybrid by using the dopant pTSA. This can also be seen for other analytes as well. Across the entire range SDS had the responded the highest followed by pTSA then no response for $LiClO_4$, L-CSA, D-CSA and bare SWNT to n-hexane. So we have increased the sensitivity to n-hexane by changing the dopant to either SDS or pTSA (see Figure 3.13).

There was also shown to be a difference between L-CSA and D-CSA. This can be seen in the gases NO_2, RH, MeOH, EtOH, and benzene (Figure 3. 10 and 3.11). It appears then there was a difference in response between the two entamories.

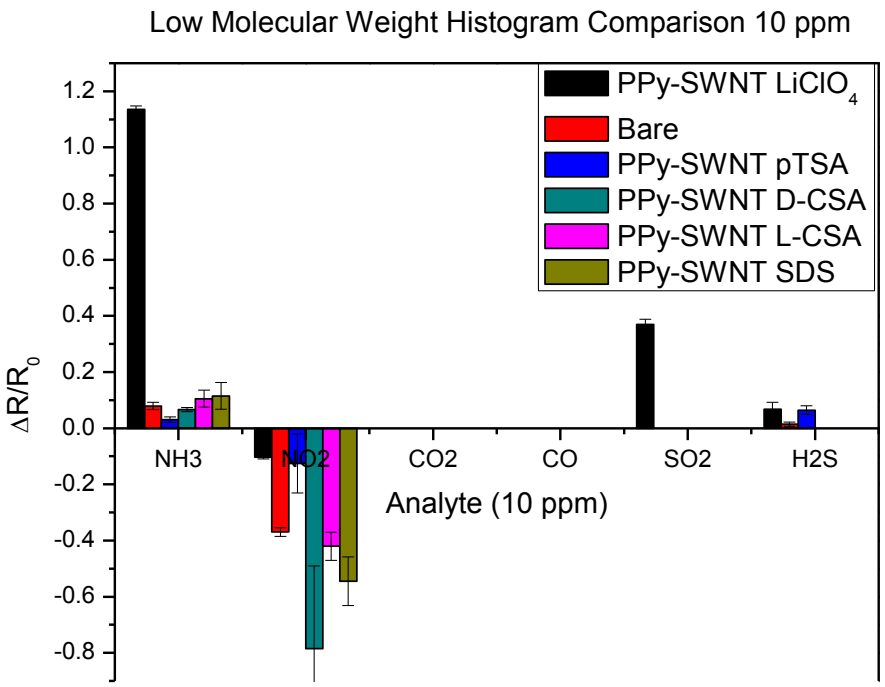

Figure 3.10 Low Molecular Weight gases response to PPy-SWNT devices with different dopants.

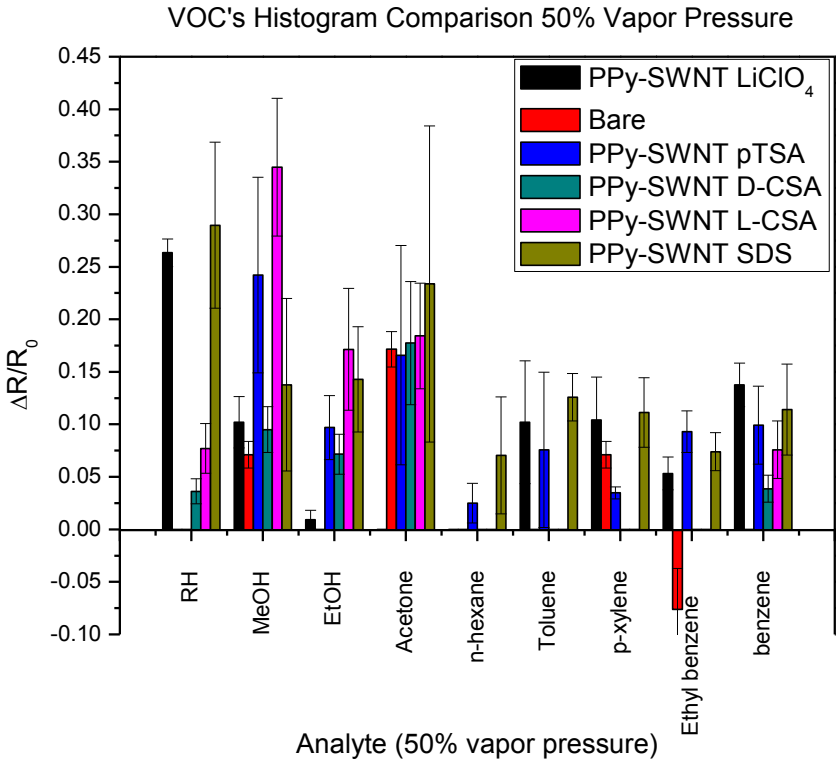

Figure 3.11 VOC's gases response to PPy-SWNT devices with different dopants.

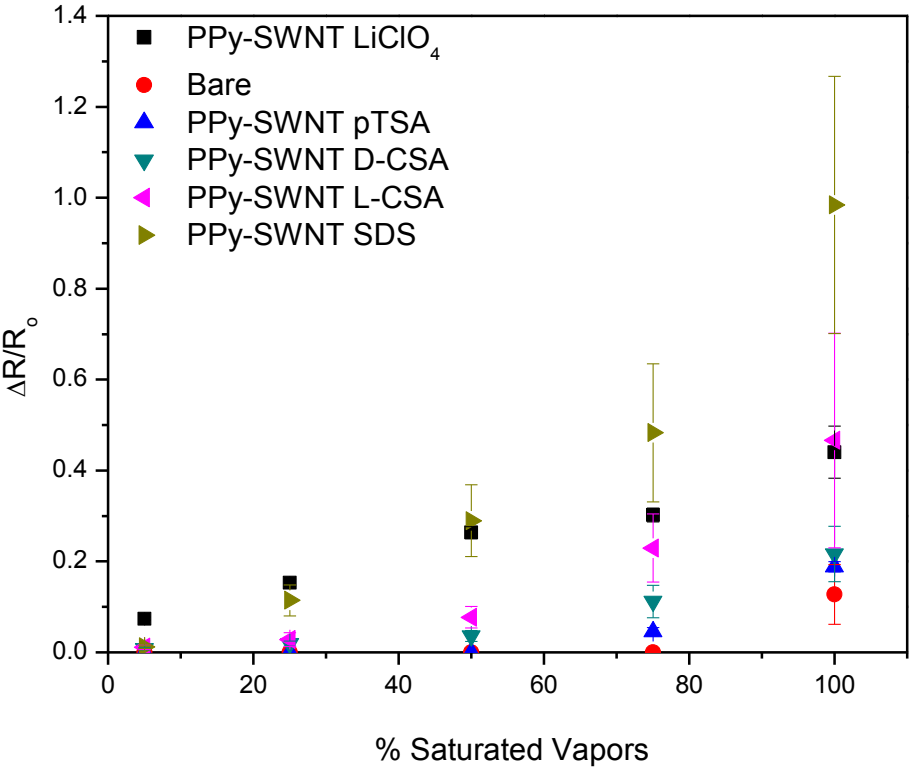

Figure 3.12 Calibration Curve of RH to PPy-SWNT with different dopants from 5 % to 100 % vapor pressure.

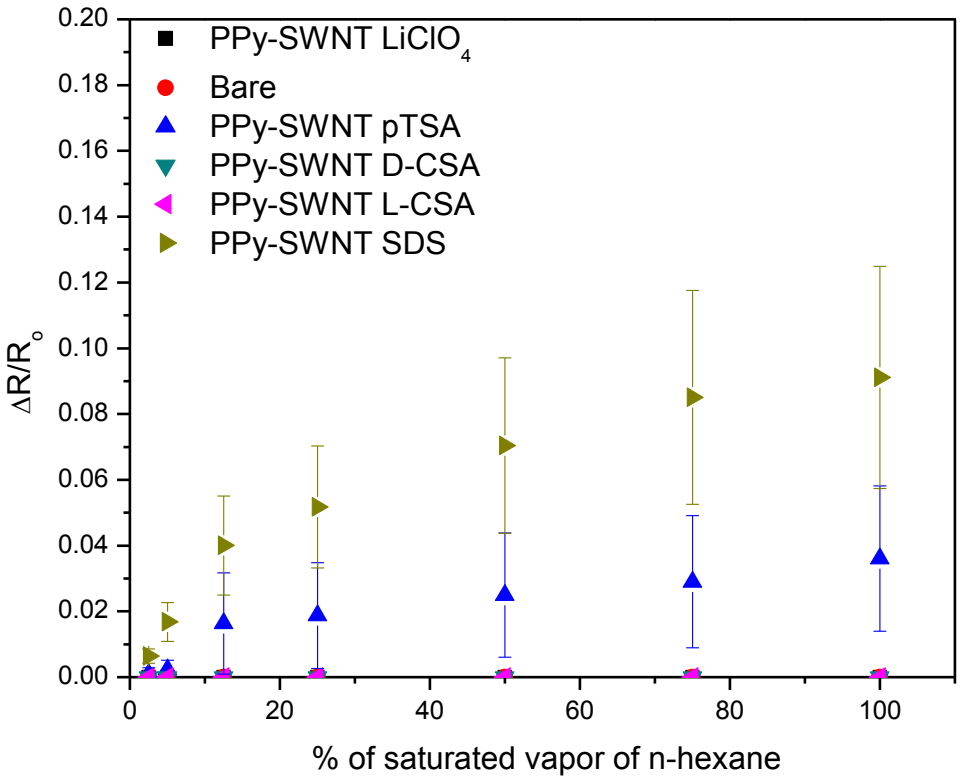

Figure 3.13 Calibration Curve of n-hexane to PPy-SWNT with different dopants from 2.5 % to 100 %.

3.2.3 Impact of Changing Dopant on PPy

Changing of the dopant in the PPy has several known impacts on the material which shape the sensing ability of the materials. First, it has been shown that as the dopant size increases the conductivity decreases. Second, as the dopant size increases the d-spacing increases as well[39]. The d-spacing determines the porosity of the PPy film[40]. Porosity is the measure of the void space in the material. Third, X-ray diffraction studies done on PPy films have shown that the dopant has a significant impact on the microstructure of films[41]. This provides a better understanding of the morphology of the material. Lastly, the linear expansion coefficient or swelling of a film due to water or any other liquid, is related to the packing density of PPy film. So as the packing density of PPy increases the amount of swelling increases[42]. All of these properties have an impact on how the material PPy responded to the gases whether they are low molecular weight gases or VOCs.

3.2.4 D-CSA vs. L-CSA

The difference between L and D-CSA was first thought to be due to the creation of optically active, or chiral PPy[43]. This was later found not to be the case when further literature review was done, and it was determined that using these two enatomeris does not lead to the creation of chiral PPy[44, 45]. On the other hand there is an obvious difference between the two when it comes to sensing. Again this can be seen for the cases of NO_2, RH, MeOH, EtOH, and benzene (Figure 3. 10 and 3.11) in how they responded.

This could be because of the interaction between the chiral SWNT and PPy itself. Further work would be needed to confirm if this is truly the source of the difference.

3.2.5 Permissible Exposure Limit (PEL) and Range of Testing

Before the other gases are discussed, the range of gases selected to be tested for the sensors needs to be addressed. In this work, for the low molecular weight gases NH_3, SO_2, CO, CO_2, H_2S, and NO_2 the range selected was PEL value divided by ten for the low and PEL value multiplied by two for the high. The range was centered on the PEL value because this is the value put forth by OSHA as the maximum that an individual should be exposed to in an eight hour period. PEL values of the low molecular weight gases are shown in Table 3.1.

Table 3.1 PEL Values of Low Molecular Weight Gases

Analyte	PEL value
NH_3	50 ppm
SO_2	5 ppm
CO	50 ppm
CO_2	5000 ppm
H_2S	20 ppm
NO_2	5 ppm[46]

Table 3.2 PEL value of the VOCs

Analyte	PEL value
Ethyl benzene	100ppm
Toluene	200ppm
p-Xylene	100ppm
Benzene	1ppm
n-Hexane	500ppm
Ethanol	1000ppm
Methanol	200ppm
Acetone	1000ppm [46]

The VOCs also have PEL values (Table 3.2). However, in the case of the VOCs the PEL values were not used as the range. Instead, the range used was the percent vapor pressure.

This was because we were not able to detect values in the range of the PEL values of these gases. The percent vapor pressure was higher than PEL value in all cases. For the VOCs the range was 2.5 % vapor pressure to 100 % vapor pressure. For a VOC such as acetone this meant that 2.5 % was equal to a value of 11,650 ppm.

Now to discuss the individual responses not all already touched upon.

3.2.6 CO and CO_2

The CO or CO_2 were tested and there was no response even at their highest values

3.2.7 SO_2

All other gases responded to at least one dopant. In the case of SO_2 the gas responded to the dopant $LiClO_4$ only (Figure 3.14).

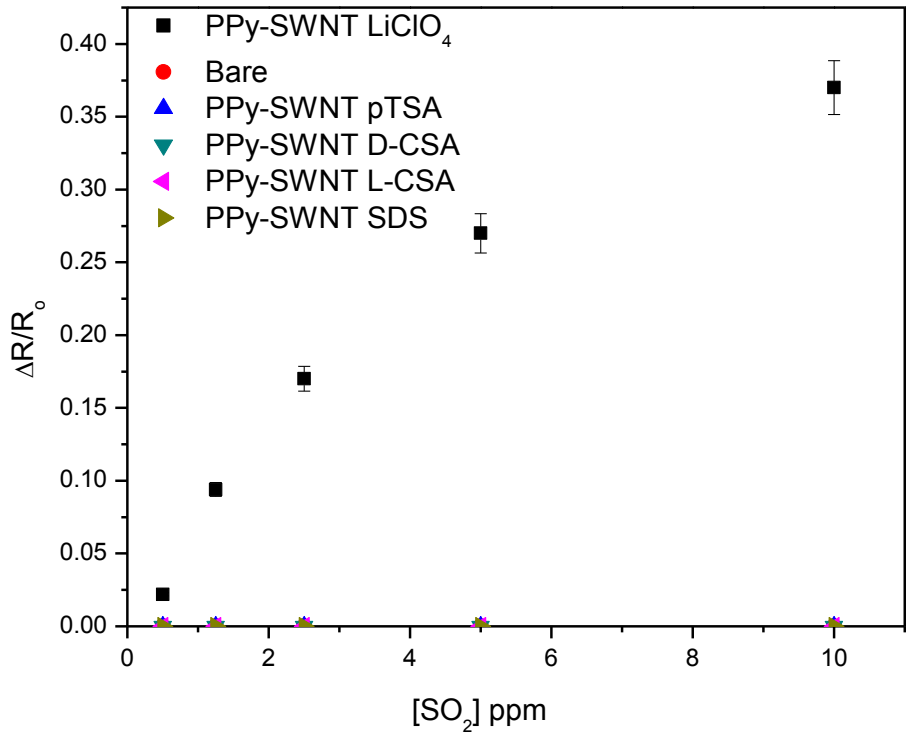

Figure 3.14 Calibration Curve of SO_2 to PPy-SWNT with different dopants from 0.5 ppm to 10 ppm.

3.2.8 NH_3

When NH_3 was exposed to the hybrids with other dopants, they all responded (Figure 3.15). The $LiClO_4$ had the highest response across the entire range compared to the other dopants. The others, while responding, clustered together across the entire range.

3.2.9 NO_2

In the case of NO_2 the response is negative. This occurs because it is an electron withdrawing species, thus resulting in more holes in the hybrid. This results in the resistance decreasing for the response[9]. All of the hybrids with the different dopants responded across the entire range. One can see the best separation of the average values at 10 ppm. At this point D-CSA has a response of ~ 80 % followed by SDS, L-CSA and bare, then pTSA and $LiClO_4$ (Figure 3.16).

3.2.10 H_2S

For H_2S only two of the dopants, $LiClO_4$ and pTSA, responded in addition to the bare SWNT. If we examine the average values at 40 ppm we can see that pTSA had the highest response ~ 14 % followed by the bare then lastly the $LiClO_4$ (Figure 3.17).

3.2.11 MeOH

In the case of MeOH, all of the dopants responded. There was very low response from 2.5 % to 25 % and clustering of the data. After this point there was more of a spread of the data. At 100 % there was a very high response and separation of the data, but this feature of the data is probably due to condensation of the analyte on the material and not

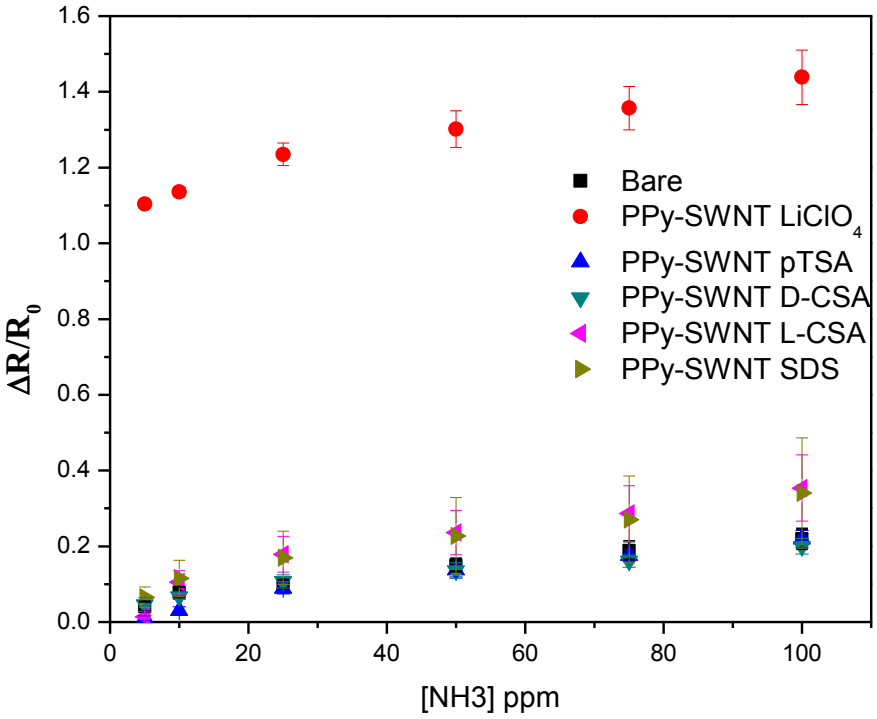

Figure 3.15 Calibration Curve of NH_3 to PPy-SWNT with different dopants from 5 ppm to 100 ppm.

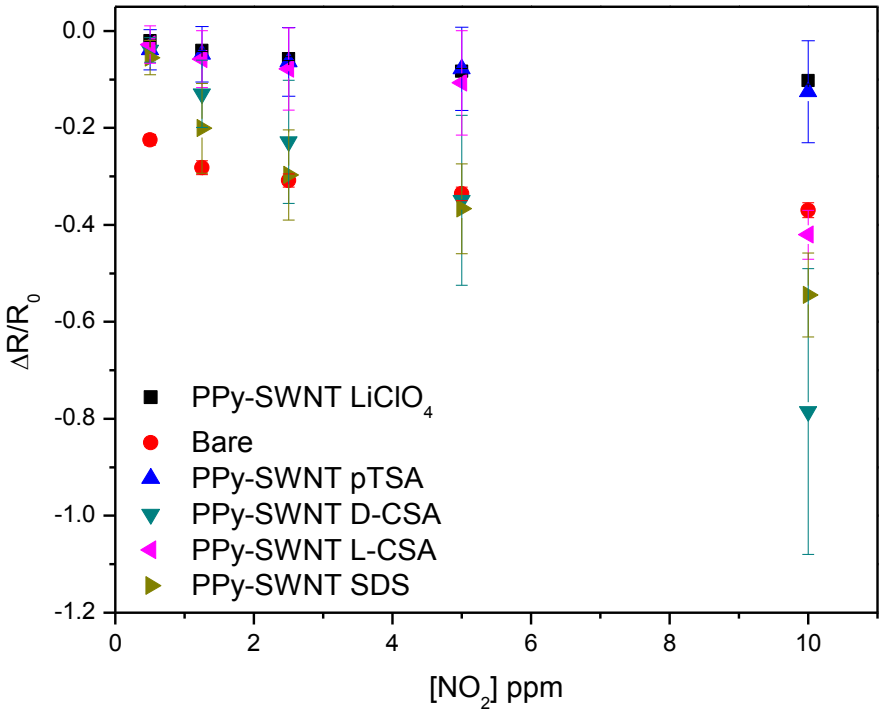

Figure 3.16 Calibration Curve of NO_2 to PPy-SWNT with different dopants from 0.5 ppm to 10

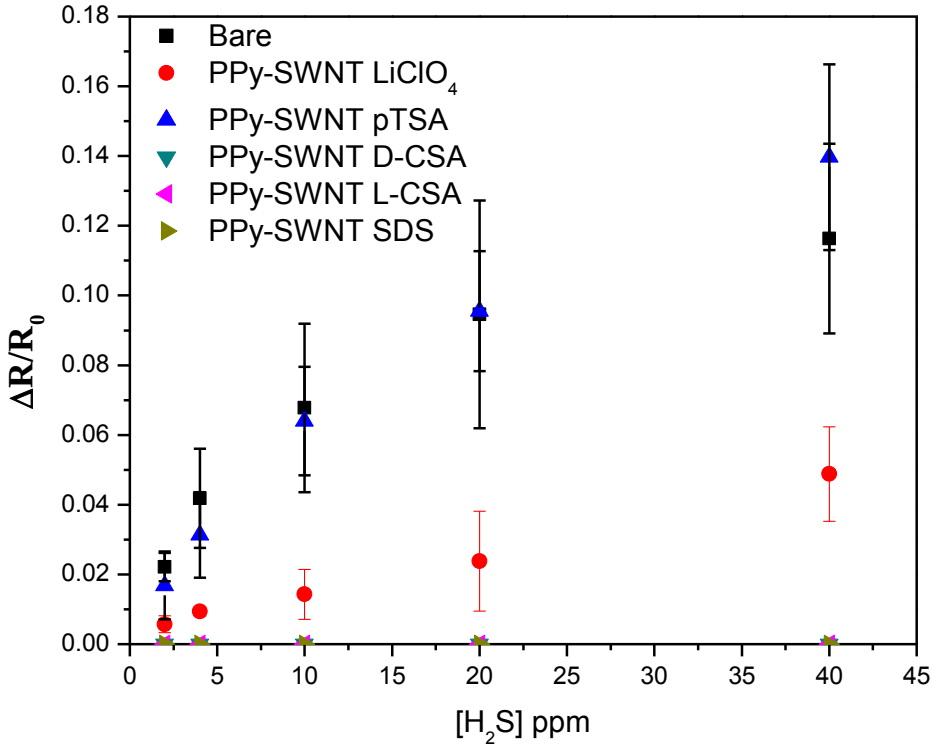

Figure 3.17 Calibration Curve of H_2S to PPy-SWNT with different dopants from 2 ppm to 40

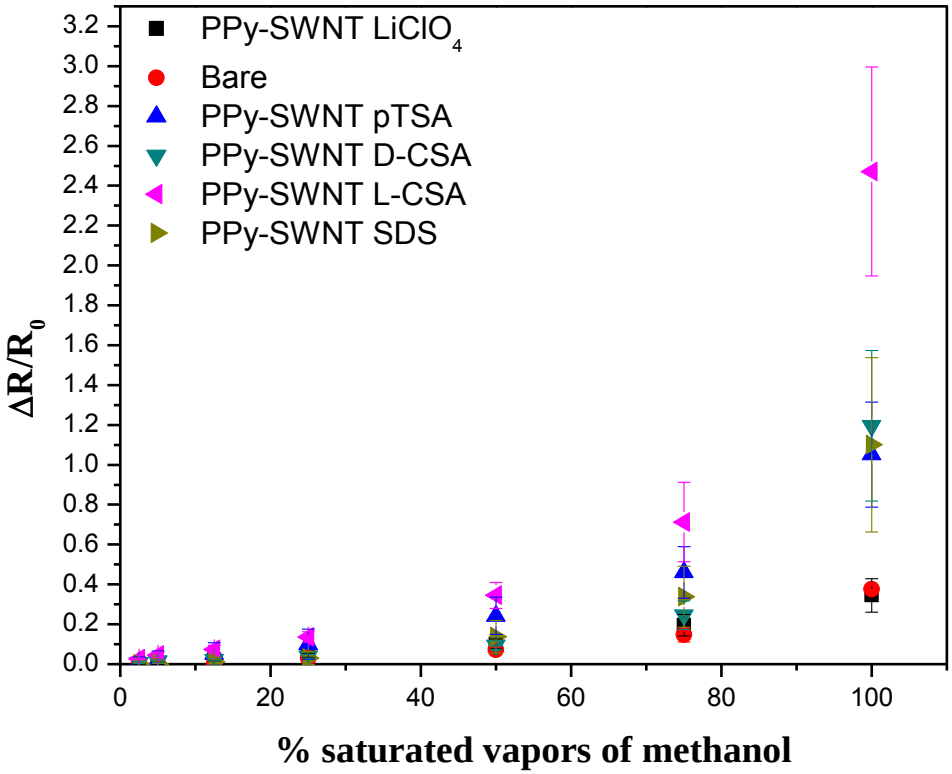

Figure 3.18 Calibration Curve of MeOH to PPy-SWNT with different dopants from 2.5% to 100%

a true response. This was an issue with most of the VOCs and RH at 100 % vapor pressure (Figure 3.18).

3.2.12 EtOH

For EtOH all of the dopants responded from 50 % onward. The bare did not respond until 100 %, which can be ignored as explained previously as being due to condensation. At less than 25 % only L-CSA, pTSA and D-CSA responded (Figure 3.19).

3.2.13 Acetone

From 2.5 % to 12.5 % there was no response for acetone except for a small response from pTSA, ~ 3 % at 12.5 %. At 25% all of the dopants including the bare started to respond except for $LiClO_4$ (Figure 3.20).

3.2.14 Toluene

For toluene only three dopants responded across the entire range these being SDS, pTSA and $LiClO_4$. They also were consistent as to which had a higher response to the other. Meaning SDS always responded higher than LiClO, followed by pTSA. This is comparing the average values SDS followed by $LiClO_4$ then by pTSA (Figure 3.21).

3.2.15 p-Xylene

In the case of p-Xylene, the same three dopants responded again as in the case of toluene, these being SDS, $LiClO_4$, and pTSA. From 12.5 % they were consistent in the amount of

the response. They were SDS and $LiClO_4$ approximately the same, followed by pTSA. Bare responded from 25 % on (Figure 3.22).

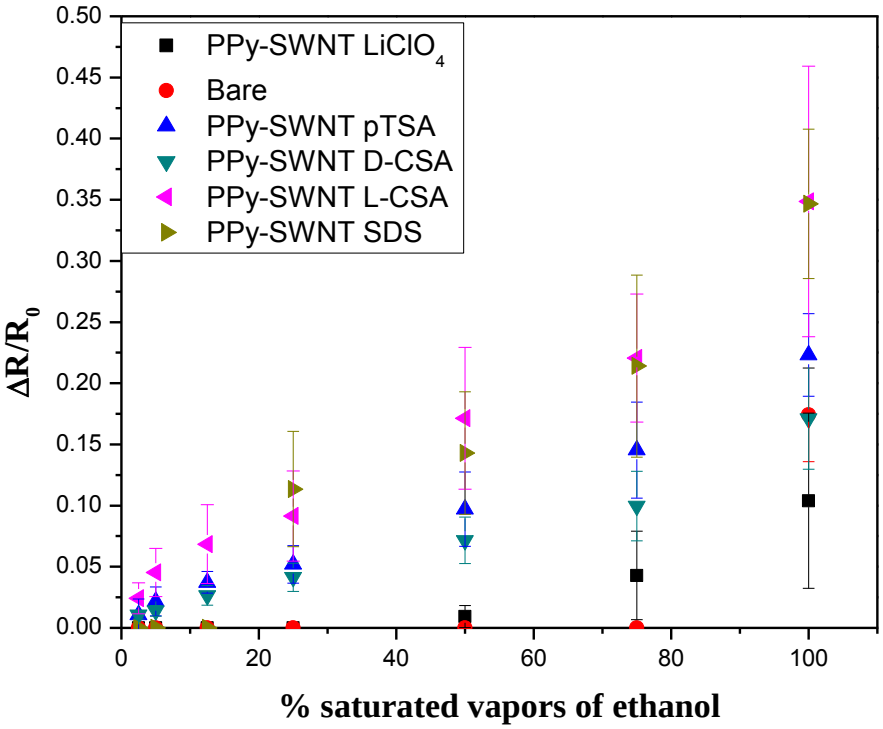

Figure 3.19 Calibration Curve of EtOH to PPy-SWNT with different dopants from 2.5 % to 100 % vapor

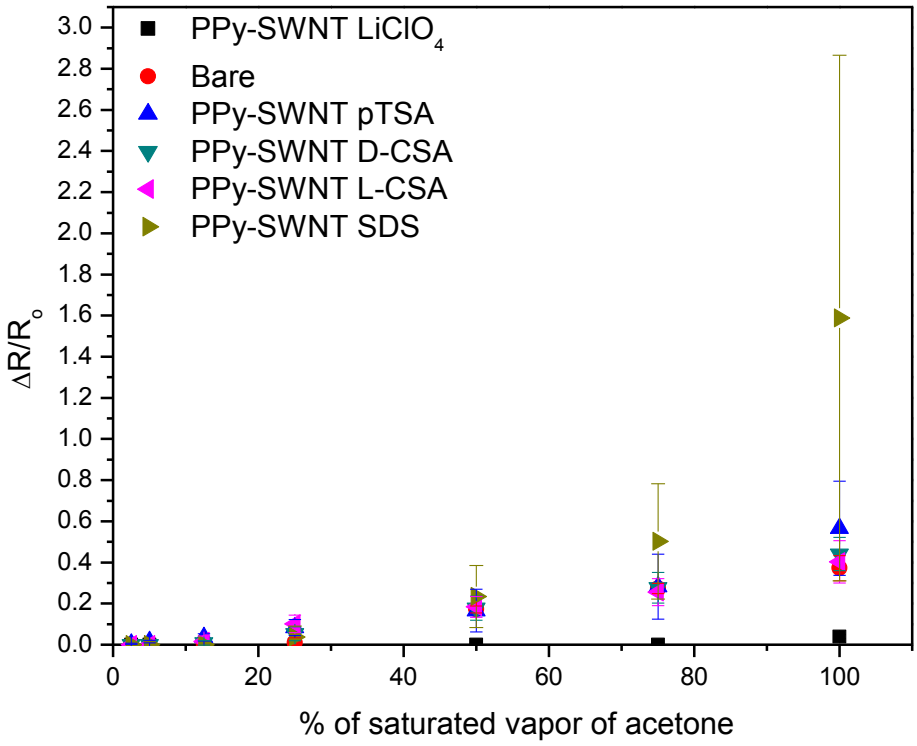

Figure 3.20 Calibration Curve of Acetone to PPy-SWNT with different dopants from 2.5 % to 100 % vapor pressure.

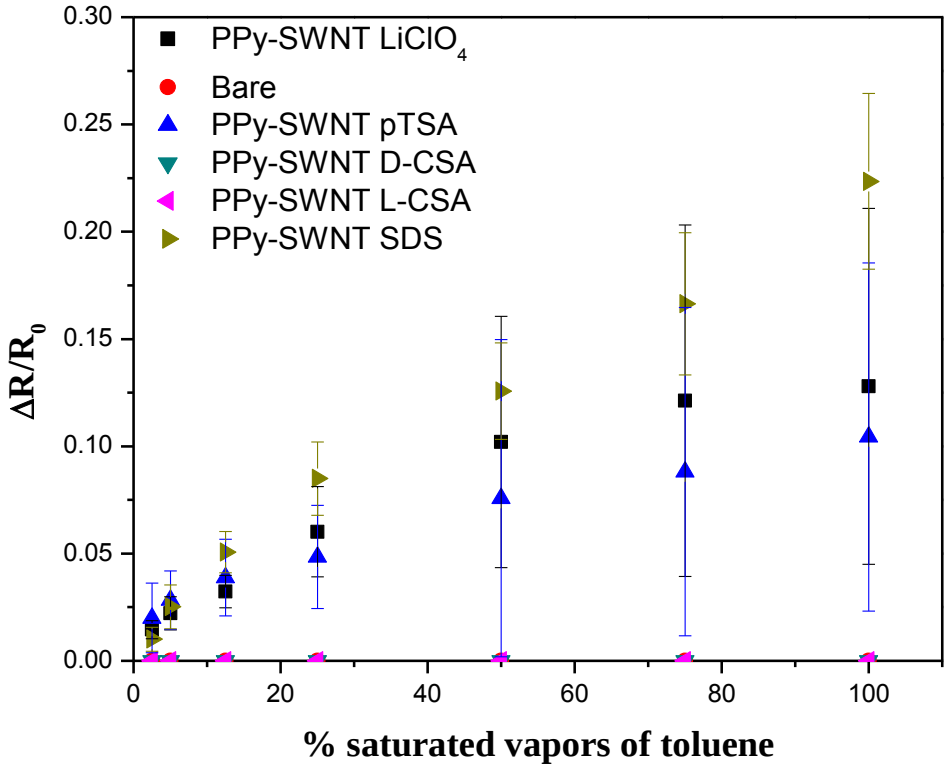

Figure 3.21 Calibration Curve of Toluene to PPy-SWNT with different dopants from 2.5 % to 100 % vapor pressure.

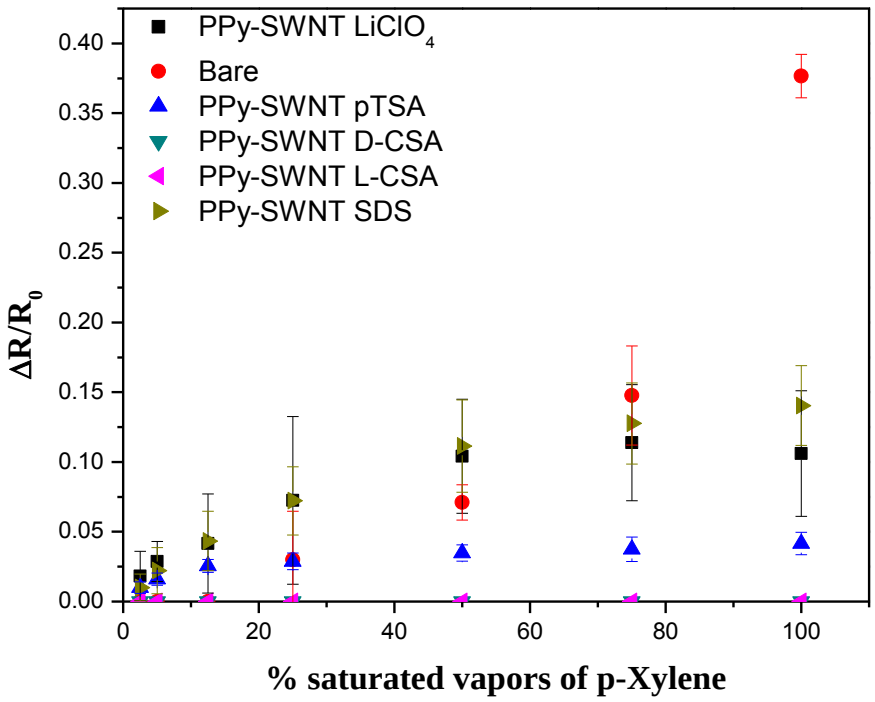

Figure 3.22 Calibration Curve of p-Xylene to PPy-SWNT with different dopants from 2.5 % to 100 % vapor pressure.

3.2.16 Ethyl Benzene

For ethyl benzene the bare responds in a negative manner while the rest of the responses are positive. The reason for this is not known at this time. The CSAs don't respond at all, but the other dopants do (Figure 3.23), these being the dopants pTSA, SDS and $LiClO_4$. Of these pTSA responds the highest on average; then from 2.5 % to 25 % $LiClO_4$ is higher than SDS. Beyond this point there is a switch; then SDS is having a higher response on average to the ethyl benzene (Figure 3.24).

3.2.17 Benzene

With benzene all of the dopants responded across the entire range. The bare did not respond at all. This is an example of great improvement of sensitivity of the hybrid over the bare SWNTs. If we look at 50 %, the responses on average are as follows: $LiClO_4$ at ~ 14 %, then SDS, pTSA, L-CSA then finally D-CSA (Figure 3.25).

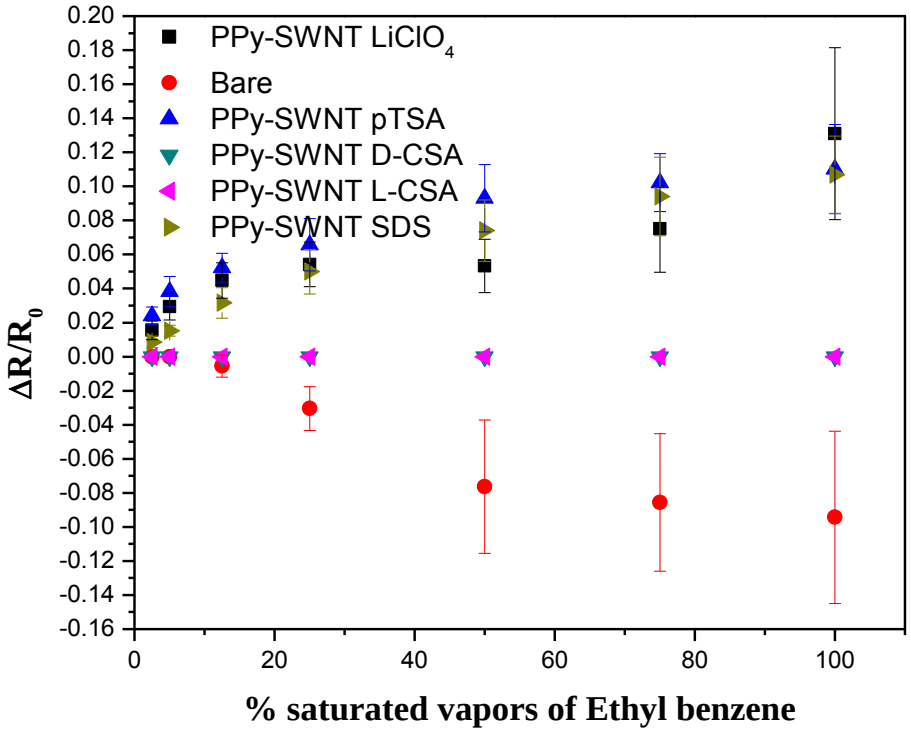

Figure 3.23 Calibration Curve of Ethyl benzene to PPy-SWNT with different dopants from 2.5 % to 100 % vapor pressure.

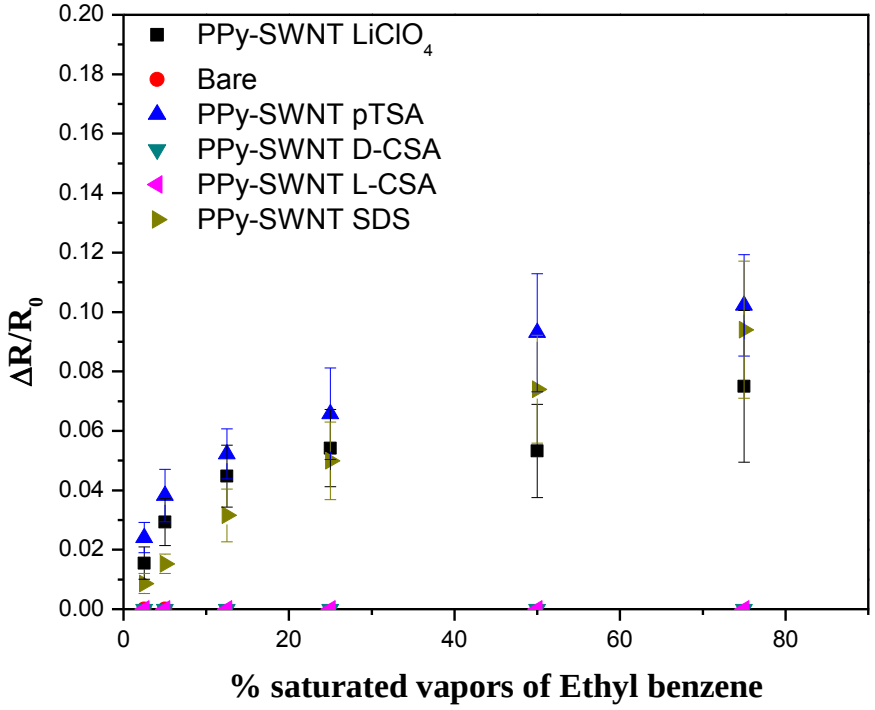

Figure 3.24 Calibration Curve of Ethyl benzene to PPy-SWNT with different dopants from 2.5 % to 100 % vapor pressure, zoom in.

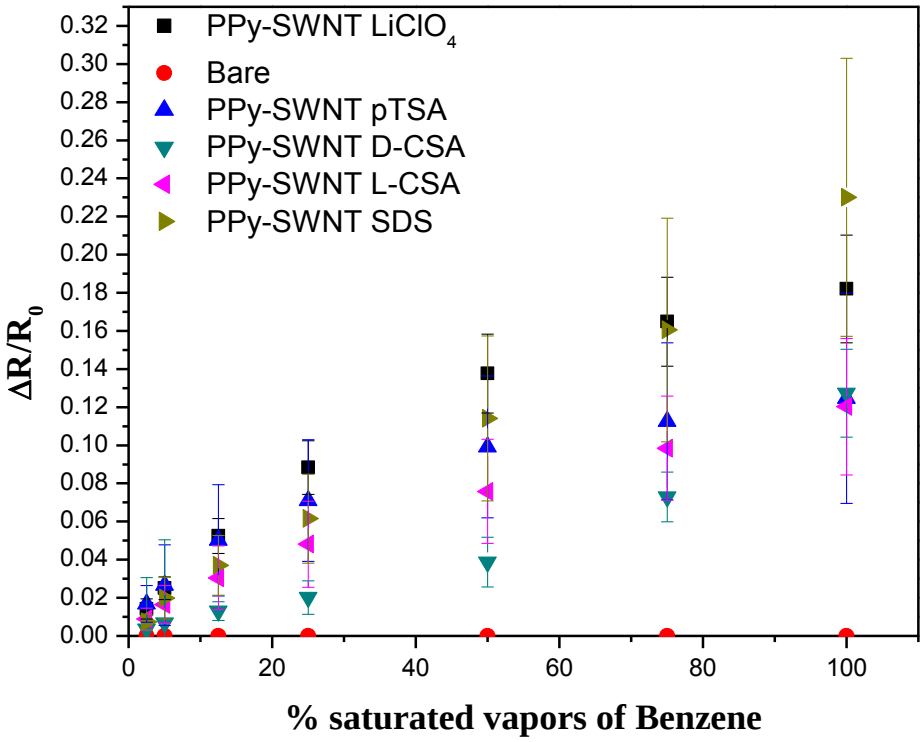

Figure 3.25 Calibration Curve of benzene to PPy-SWNT with different dopants from 2.5 % to 100 % vapor pressure.

CHAPTER 4: CONCLUSION

4.1 Ammonia Gas Sensor Optimization

In summary, it has been shown that PPy-SWNT-bundle hybrids made electrochemically can be used as gas sensors that are reproducible, modify the limit of detection, and show increased sensitivity between the bare and the 1 μC PPy-SWNT-bundle hybrid. Also, the mechanism of sensing was explored and has been shown to be a gate effect in the case of the 1 μC PPy-SWNT-bundle hybrid. This is in contrast to literature systems in which the mechanism was a Schottky effect. This system was made up of exclusively of semiconducting SWNT while this works system is made up of a mixture of metallic and semiconducting SWNT.

The research plan as stated was to develop a PPy-SWNT sensor with $LiClO_4$ as the dopant through the optimization of thickness, by changing the charge that the PPy is applied. The sensor will be optimized for response against the gas NH_3. After this is done the optimized sensor will then be tested against different analytes. This will give a pattern of response. These main goals were accomplished.

4.2 Changing of the Dopant

In summary, this research explored the impact of changing the dopant on the selectivity and sensitivity of PPy-SWNT from $LiClO_4$ to the other dopants, SDS, L-CSA, D-CSA, and pTSA. Also the bare was always used as a comparison. In all cases changing the dopant changed the amount of response. Simply by changing the counterion and keeping all else constant one can create an array of responses that either increases or decreases the

amount of response for the particular analytes of interest. In this research, these analytes were the low molecular weight compounds i.e. NH_3, SO_2, CO, CO_2, H_2S, and NO_2, and the VOCs, i.e. MeOH, EtOH, acetone, n-hexane, benzene, toluene, ethyl benzene, and p-xylene and RH. In case of the VOCs we were able to modulate the sensitivity of the response but not able to lower it enough, as in the case low molecular weight compounds, to the PEL level. Also we were not able to detect with any of the dopants the gases CO and CO_2. Also selectivity was found between the L-CSA and D-CSA. The difference for which is not understood at this time. Further work will have to be done to overcome these issues.

The research plan as stated was to develop new PPy-SWNT sensors, by using the same conditions, but changing the dopant. This will have the impact of changing the pattern of response of the new sensors by changing the sensitivity and selectivity. This goal was accomplished in this research.

References

1. Mubeen, S.; Zhang, T.; Yoo, B.; Deshusses, M. A.; Myung, N. V., Palladium nanoparticles decorated single-walled carbon nanotube hydrogen sensor. *Journal of Physical Chemistry C* **2007,** 111, (17), 6321-6327.

2. Wilson, A.; Baietto, M., Applications and Advances in Electronic-Nose Technologies. *Sensors* **2009,** 9, (7), 5099-5148.

3. Douglas A. Skoog, F. J. H., Timothy A. Nieman, *Principles of Instrumental Analysis*. 5th ed.; Saunders College Publishing: Philadelphia, 1998.

4. Appl, M., Ammonia. In *Ullmann's Encyclopedia of Industrial Chemistry*, Wiley-VCH Verlag GmbH & Co. KGaA: Weinheim, 2006; pp 1-155.

5. USGS NITROGEN (FIXED)—AMMONIA. http://minerals.usgs.gov/minerals/pubs/commodity/nitrogen/mcs-2009-nitro.pdf

6. OSHA Safety and Health Topics: Ammonia http://www.osha.gov/dts/chemicalsampling/data/CH_218300.html

7. Iijima, S., Helical microtubules of graphitic carbon. *Nature* **1991,** 354, (6348), 56-58.

8. Dresselhaus M.S., D. G., Eklund P.C., *Science of Fullerenes and Carbon Nanotubes*. Academic Press: San Diego, 1996.

9. Kong, J.; Franklin, N. R.; Zhou, C. W.; Chapline, M. G.; Peng, S.; Cho, K. J.; Dai, H. J., Nanotube molecular wires as chemical sensors. *Science* **2000,** 287, (5453), 622-625.

10. Snow, E. S.; Perkins, F. K.; Houser, E. J.; Badescu, S. C.; Reinecke, T. L., Chemical detection with a single-walled carbon nanotube capacitor. *Science* **2005,** 307, (5717), 1942-1945.

11. Li, J.; Lu, Y. J.; Ye, Q.; Cinke, M.; Han, J.; Meyyappan, M., Carbon nanotube sensors for gas and organic vapor detection. *Nano Letters* **2003,** 3, (7), 929-933.

12. Dai, H. J., Carbon nanotubes: opportunities and challenges. *Surface Science* **2002,** 500, (1-3), 218-241.

13. Yu, Z.; Li, S. D.; Burke, P. J., Synthesis of aligned arrays of millimeter long, straight single-walled carbon nanotubes. *Chemistry of Materials* **2004,** 16, (18), 3414-3416.

14. Baughman, R. H.; Zakhidov, A. A.; de Heer, W. A., Carbon nanotubes - the route toward applications. *Science* **2002,** 297, (5582), 787-792.

15. Ellison, M. D.; Crotty, M. J.; Koh, D.; Spray, R. L.; Tate, K. E., Adsorption of NH3 and NO2 on single-walled carbon nanotubes. *Journal of Physical Chemistry B* **2004,** 108, (23), 7938-7943.

16. Quang, N. H.; Van Trinh, M.; Lee, B. H.; Huh, J. S., Effect of NH3 gas on the electrical properties of single-walled carbon nanotube bundles. *Sensors and Actuators B-Chemical* **2006,** 113, (1), 341-346.

17. Pengfei, Q. F.; Vermesh, O.; Grecu, M.; Javey, A.; Wang, O.; Dai, H. J.; Peng, S.; Cho, K. J., Toward large arrays of multiplex functionalized carbon nanotube sensors for highly sensitive and selective molecular detection. *Nano Letters* **2003,** 3, (3), 347-351.

18. Lee, C. Y.; Sharma, R.; Radadia, A. D.; Masel, R. I.; Strano, M. S., On-chip micro gas chromatograph enabled by a noncovalently functionalized single-walled carbon nanotube sensor array. *Angewandte Chemie-International Edition* **2008,** 47, (27), 5018-5021.

19. Zhang, T.; Mubeen, S.; Yoo, B.; Myung, N. V.; Deshusses, M. A., A gas nanosensor unaffected by humidity. *Nanotechnology* **2009,** 20, (25), 5.

20. Kauffman, D. R.; Star, A., Carbon nanotube gas and vapor sensors. *Angewandte Chemie-International Edition* **2008,** 47, (35), 6550-6570.

21. Cui, Y.; Duan, X.; Huang, Y.; Lieber, C. M., In *Metals and semiconductor nanowires*, Z.L., W., Ed. Kluwer Academic Publishers: Boston, MA, 2003; Vol. 1, pp 3-68.

22. Skotheim, T. A., *Handbook of Conducting Polymers*. Marcel Dekker, Inc.: New York, 1986; Vol. 1.

23. Jones, E. T. T.; Chyan, O. M.; Wrighton, M. S., PREPARATION AND CHARACTERIZATION OF MOLECULE-BASED TRANSISTORS WITH A 50-NM SOURCE-DRAIN SEPARATION WITH USE OF SHADOW DEPOSITION TECHNIQUES - TOWARD FASTER, MORE SENSITIVE MOLECULE-BASED DEVICES. *Journal of the American Chemical Society* **1987,** 109, (18), 5526-5528.

24. Paul, E. W.; Ricco, A. J.; Wrighton, M. S., RESISTANCE OF POLYANILINE FILMS AS A FUNCTION OF ELECTROCHEMICAL POTENTIAL AND THE FABRICATION OF POLYANILINE-BASED MICROELECTRONIC DEVICES. *Journal of Physical Chemistry* **1985,** 89, (8), 1441-1447.

25. Bidan, G., ELECTROCONDUCTING CONJUGATED POLYMERS - NEW SENSITIVE MATRICES TO BUILD UP CHEMICAL OR ELECTROCHEMICAL SENSORS - A REVIEW. *Sensors and Actuators B-Chemical* **1992,** 6, (1-3), 45-56.

26. Kharat, H. J.; Kakde, K. P.; Savale, P. A.; Datta, K.; Ghosh, P.; Shirsat, M. D., Synthesis of polypyrrole films for the development of ammonia sensor. *Polymers for Advanced Technologies* **2007,** 18, (5), 397-402.

27. Brie, M.; Turcu, R.; Neamtu, C.; Pruneanu, S., The effect of initial conductivity and doping anions on gas sensitivity of conducting polypyrrole films to NH3. *Sensors and Actuators B-Chemical* **1996,** 37, (3), 119-122.

28. Carquigny, S.; Sanchez, J. B.; Berger, F.; Lakard, B.; Lallemand, F., Ammonia gas sensor based on electrosynthesized polypyrrole films. *Talanta* **2009,** 78, (1), 199-206.

29. Collins, G. E.; Buckley, L. J., Conductive polymer-coated fabrics for chemical sensing. *Synthetic Metals* **1996,** 78, (2), 93-101.

30. Su, P. G.; Lee, C. T.; Chou, C. Y., Flexible NH3 sensors fabricated by in situ self-assembly of polypyrrole. *Talanta* **2009,** 80, (2), 763-769.

31. Ameer, Q.; Adeloju, S. B., Polypyrrole-based electronic noses for environmental and industrial analysis. *Sensors and Actuators B-Chemical* **2005,** 106, (2), 541-552.

32. Jang, J., Conducting polymer nanomaterials and their applications. In *Emissive Materials: Nanomaterials*, Springer-Verlag Berlin: Berlin, 2006; Vol. 199, pp 189-259.

33. Bai, H.; Shi, G. Q., Gas sensors based on conducting polymers. *Sensors* **2007,** 7, (3), 267-307.

34. Zhang, T.; Nix, M. B.; Yoo, B. Y.; Deshusses, M. A.; Myung, N. V., Electrochemically functionalized single-walled carbon nanotube gas sensor. *Electroanalysis* **2006,** 18, (12), 1153-1158.

35. In *Physics: Calucus 2nd Edition*, Hecht, E., Ed. Brooks/Cole Thomson Learning: Pacific Grove, CA 2000; pp 867-868.

36. Heller, I.; Janssens, A. M.; Mannik, J.; Minot, E. D.; Lemay, S. G.; Dekker, C., Identifying the mechanism of biosensing with carbon nanotube transistors. *Nano Letters* **2008,** 8, (2), 591-595.

37. Peng, N.; Zhang, Q.; Chow, C. L.; Tan, O. K.; Marzari, N., Sensing Mechanisms for Carbon Nanotube Based NH3 Gas Detection. *Nano Letters* **2009,** 9, (4), 1626-1630.

38. Skakalova, V.; Kaiser, A. B.; Woo, Y. S.; Roth, S., Electronic transport in carbon nanotubes: From individual nanotubes to thin and thick networks. *Physical Review B* **2006,** 74, (8), 10.

39. Yamaura, M.; Hagiwara, T.; Iwata, K., Enhancement of electrical conductivity of polypyrrole film by stretching: Counter ion effect. *Synthetic Metals* **1988,** 26, (3), 209-224.

40. Deore, B. C., Zhidong; Nagaoka, Tsutomu, overoxidized polypyrrole with dopant complementary cavities as a new molecular imprinted polymer matrix. *The Japan Society for Analytical Chemistry* **1999,** 15, 827-828.

41. Warren, L. F.; Walker, J. A.; Anderson, D. P.; Rhodes, C. G.; Buckley, L. J., A Study of Conducting Polymer Morphology. *Journal of The Electrochemical Society* **1989,** 136, (8), 2286-2295.

42. Okuzaki, H.; Kuwabara, T.; Kondo, T., Role and effect of dopant ion on sorption-induced motion of polypyrrole films. *Journal of Polymer Science Part B: Polymer Physics* **1998,** 36, (14), 2635-2642.

43. Zhou, Y.; Yu, B.; Zhu, G., Electropolymeric generation of optically active polypyrrole. *Polymer* **1997,** 38, (21), 5493-5495.

44. Qu, L.; Shi, G.; Yuan, J.; Han, G.; Chen, F. e., Preparation of polypyrrole microstructures by direct electrochemical oxidation of pyrrole in an aqueous solution of camphorsulfonic acid. *Journal of Electroanalytical Chemistry* **2004,** 561, 149-156.

45. Aboutanos, V. A., P.; Kane-Maguire, L. A. P.; Wallace, G. G., Optically Active Polypyrroles Containing Chiral Dopant Anions. *Australian Journal of Chemistry* **2000,** 53, 83-87.

46. Standards, O. S. a. H. TABLE Z-1 LIMITS FOR AIR CONTAMINANTS. http://www.osha.gov/pls/oshaweb/owadisp.show_document?p_table=STANDARDS&p_id=9992&p_text_version=FALSE